THE STUDY OF PHOTOCHEMICAL INTERMEDIATES OF SELECTED ORGANOMETALLIC COMPOUNDS

by

WENJIA XIA

THESIS SUBMITTED IN PARTIAL FULFILLMENT OF

THE REQUIREMENTS FOR THE DEGREE OF

MASTER OF SCIENCE

in the Department

of

Chemistry

SIMON FRASER UNIVERSITY

December, 1990

APPROVAL

Name: WENJIA XIA

Degree: MASTER OF SCIENCE

Title of Thesis: THE STUDY OF PHOTOCHEMICAL INTERMEDIATES OF SELECTED ORGANOMETALLIC COMPOUNDS

Examining Committee:

Chair: Dr. P. Percival

Dr. R. H. Hill
Senior Supervisor

Dr. L. K. Peterson
Supervisory Committee

Dr. Y. L. Chow
Supervisory Committee

Dr. F. W. B. Einstein
Internal Examiner

Date Approved: December 1990

PARTIAL COPYRIGHT LICENSE

I hereby grant to Simon Fraser University the right to lend my thesis, project or extended essay (the title of which is shown below) to users of the Simon Fraser University Library, and to make partial or single copies only for such users or in response to a request from the library of any other university, or other educational institution, on its own behalf or for one of its users. I further agree that permission for multiple copying of this work for scholarly purposes may be granted by me or the Dean of Graduate Studies. It is understood that copying or publication of this work for financial gain shall not be allowed without my written permission.

Title of Thesis/Project/Extended Essay

THE STUDY OF PHOTOCHEMICAL INTERMEDIATES OF SELECTED ORGANOMETALLIC COMPOUNDS

Author: ___
(signature)

WENJIA XIA
(name)

Dec. 18, 1992
(date)

Abstract:

The photochemistry of selected four-legged piano stool molecules has been studied. The reactivities and geometries of the primary photoproducts have been ellucidated by means of both experimental and theoretical methods.

The photochemistry of molecules of the type $CpM(CO)_2XL$ ($Cp=\eta^5$-C_5H_5, M=V, X=L=PR_3; M=W, X=Cl,I, L=PR_3) has been investigated. In each case, the photoreaction has been studied at temperatures as low as 12 K by FTIR spectroscopy. For molecules of the type cis or trans $CpV(CO)_2L_2$, L=$P(OMe)_3$, $P(OEt)_3$, photolysis resulted in a distinct CO loss product depending on the stereochemistry of the starting complexes. This intermediate reacted with CO to regenerate the substrate in its original geometry during the thermal back reaction. In contrast, complexes such as cis or trans $CpW(CO)_2IL$, L=$P(OMe)_3$, PPh_3, $P(nBu)_3$, show temperature dependent intermediates. At 12K they behave the same as the Vanadium compounds. However, at 77k, the intermediates isomerize resulting in generation of a mixture of both the cis and trans compounds during the thermal back reaction with CO.

In order to correctly analyze and assign the above FTIR data, particularly the geometries of the photochemical intermediates, two theoretical methods were used. The first one involved qualitative and semiquantitative inferences from force constant theory based on the "frequency factored force field" as to the signs and relative magnitudes of CO stretching force constants and stretching-stretching interaction force constants. The ligand effect force constants were calculated by using Timney's method. Based on the optimized

ligand effect constants, we were able to predict the geometries of the intermediates by assuming that the one which gives the best agreement between observed and calculated frequencies (or force constants) is the correct geometry.

The second theoretical method used was Extended Huckel Molecular Orbital calculations. EHMO method was applied to a hypothetical molecule $CpV(CO)(PPh_3)_2$ with a metal d^4 configuration. The conformational preferences, and valence molecular orbital interaction are described in detail. The minimum barrier for isomerization between the two isomers of the formula $CpV(CO)(PPh_3)_2$ was calculated to be approximately 8KJ at 12K.

DEDICATION

TO MY PARENTS

TO MY HUSBAND

ACKNOWLEDGMENTS

The author wishes to express her gratitude to:

Dr. R. H. Hill for his continuous encouragement and guidance during the course of this project.

Dr. A. Becalska and B. Palmer for their valuable help and friendship.

The generous financial support from the Natural Science and Engineering Research Council of Canada, Simon Fraser University and Dr. R. H. Hill is gratefully acknowledged.

Thanks to my husband Yu for everything.

TABLE OF CONTENTS

LIST OF TABLES

LIST OF FIGURES

LIST OF ABBREVIATIONS

Cp —— η^5-C_5H_5

Cp^* —— $\eta^5C_5Me_5$

L —— two electron donor ligands, e.g. phosphines and phosphites

X —— halogens

CT —— charge transfer

FTIR —— fourier transform infrared

IR —— infrared

UV —— ultraviolet

R —— alkyl group

EHMO —— extended Huckel molecular orbital

EFFF —— energy factored force field

Obsd —— observed

Calcd —— calculated

Diff —— difference

HOMO —— highest occupied molecular orbital

LUMO —— lowest unoccupied molecular orbital

LCAO —— linear combination of atomic orbitals

Chapter 1: Introduction

1.1 Background chemistry on four-legged piano-stool molecules

As defined in one of Poli's works[1], "four-legged piano stool" is the commonly used term for structures of type I - III (Fig.1-1). These contain a π-bonded cyclopolyene or cyclopolyenyl ligand and four additional σ-bonded two-electron-donor ligands (L).

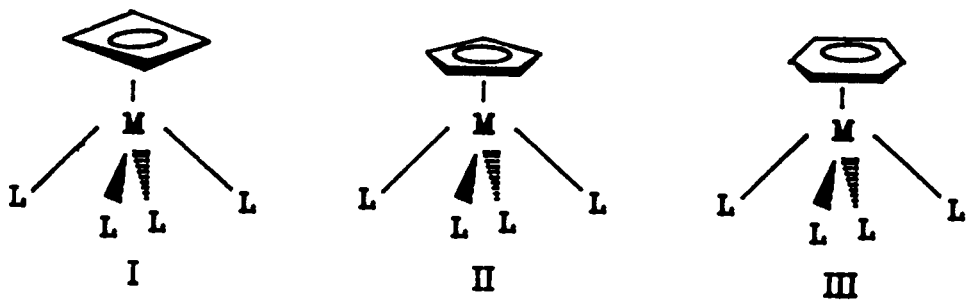

Fig.1-1: The structures of typical four-legged piano stool molecules

In a four-legged piano stool geometry, the basal positions are occupied by the four ligands and the center of the mass of the cyclopolyene or cyclopolyenyl ligand occupies the apical position. The structures may also be viewed as pseudo square pyramidal (sp) if the π-bonded ligand is considered to occupy a single coordination position.

There are several studies on four-legged piano stool molecules, both experimental and theoretical. The chemical reactivities and kinetic aspects have been studied extensively by the experimental chemists, while theoreticians put emphasis on molecular geometrical studies. For example, the photolability of $CpV(CO)_4$ has been employed in preparing a variety of $CpV(CO)_{4-n}L_n$ in the presence of a ligand, L[2-5]. Kinetic studies of the thermal substitution reactions of $CpV(CO)_4$ with a variety of phosphines and phosphites have suggested that the reaction proceeds by a dissociative pathway in which loss of a CO ligand is the rate determining step[6]. A theoretical analysis of $CpML_4$ compounds has been presented by Hoffmann[7] in which the preference for the piano-stool structure, over other possible structural isomers (isomeric pseudo-square pyramidal or pseudo-trigonal bipyramidal), was rationalized. The distortion of the Cp ring (tilting toward a η^3, η^2 conformation), which is sometimes observed experimentally, was also discussed.

Within this thesis I will use both experimental and theoretical approaches to gain some insight into the thermal and photochemical reactions of four legged piano-stool molecules. The following sections (1.2-1.5) contain brief descriptions of the techniques which will be encountered in the bulk of the thesis. Finally, in section 1.6, the research plan we set out to investigate some four-legged piano stool molecules will be described.

1.2 Some basic aspects of organometallic photochemistry

Photochemical reactions are ways by which chemical systems degrade energy that has been supplied to them in the form of light. In a sense, this is the first law of photochemistry[8], which establishes that only the radiation absorbed by the system is effective in inducing photochemical changes. Once the photonic energy has been absorbed by the molecule, this energy can be degraded in a variety of processes that induce chemical or physical changes. These processes have been named primary photochemical processes when they comprise the series of events starting with the absorption of light by a molecule and ending with the disappearance of the molecule or its conversion to a state where its reactivity is statistically no greater than that of similar molecules in thermal equilibrium with their surroundings[9].

As a result of the processes of light absorption by the molecule, it enters an excited state. The electronic transitions which are reasonable for this state can be classified as metal centered (d->d or f->f transition), charge transfer (CT), or ligand centered,. Fig.1-2 shows the electronic transitions in an octahedral coordination complex[10].

The classification mentioned above is based on the assumption that molecular orbitals in these complexes have very large contributions from either metal or ligand orbitals as one would expect for highly ionic complexes. Most organometallic complexes are covalent compounds, hence, the mixing of ligand character in the d

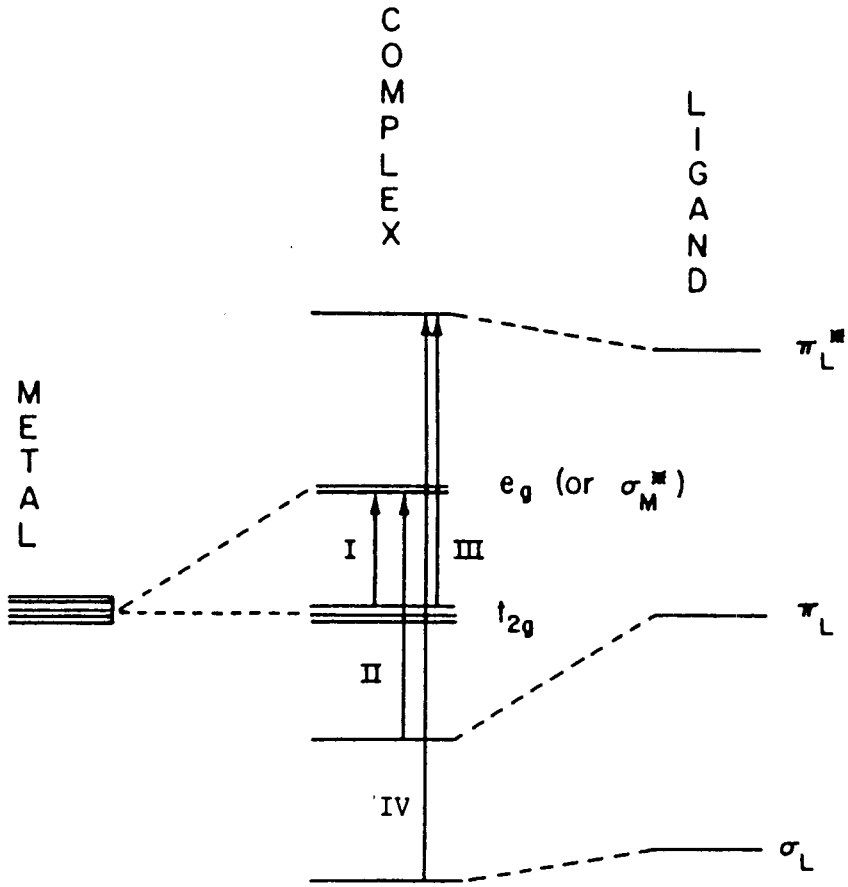

Fig. 1-2: Electronic transition in an octahedral coordination complex: (I) metal centered, (II) charge transfer ligand to metal, (III) charge transfer metal to ligand, and (IV) ligand centered.

orbitals has an important effect on the transition character in the d orbitals has an important effect on the transition probabilities. So the "metal centered" d orbitals have considerable ligand character and transitions within these orbitals are often referred to as "ligand field" instead of "metal centered".

The compounds which I studied were all metal carbonyls. The bonding between CO and open-shell d^1-d^9 transition metal ions involves both a large π back bonding, associated with the delocalization of metal $d\pi$ electrons into empty antibonding π orbitals of the CO, and a large σ donation, from filled orbitals of the CO that interact with empty metal orbitals of appropriate symmetry. Such electronic effects make the carbonyls very covalent compounds[11,12]. There are a number of electronic excited states that are available upon excitation of transition metal carbonyls resulting in a very rich photochemistry. The photochemical loss of CO, which we studied the most, is induced by population of a ligand field state of carbonyl compounds[13].

1.3 The use of cryogenics and FTIR to investigate reaction intermediates

The method used here to investigate the reaction intermediates is derived from the so-called matrix isolation method[14]. The principle behind the matrix isolation method is the following. If a reactive or unstable species is trapped in a rigid, chemically inert solid at sufficiently low temperature, then its lifetime may be extended almost indefinitely. It is unable to diffuse through the solid matrix if the latter is rigid enough and the temperature sufficiently low, and will not therefore react with other species in the matrix, nor will the alternate decay pathway, unimolecular decomposition, be allowed. Fig.1-3 shows a schematic of the experimental arrangement. The matrix is supported on a salt window (usually CsI or KBr, we use CaF_2 in our lab) clamped in a metal holder attached to a refrigeration source. This may be a dewar containing liquid H_2 (20K) or liquid He (4K) or liquid N_2 (77K), or in our lab, a closed cycle refrigerator which can operate at any temperature from about 10K to 300K. The entire sample is kept under high vacuum (about 10^{-7} Torr) and the matrix may be spectroscopically examined by placing the cell in the sample beam of an IR or UV/vis (in our case, a FTIR) spectrometer.

An ideal matrix is one which is transparent in the regions needed for spectral examination, and the inert gases, methane and N_2 have been extensively used. These are transparent in the IR and all through the visible and near UV.

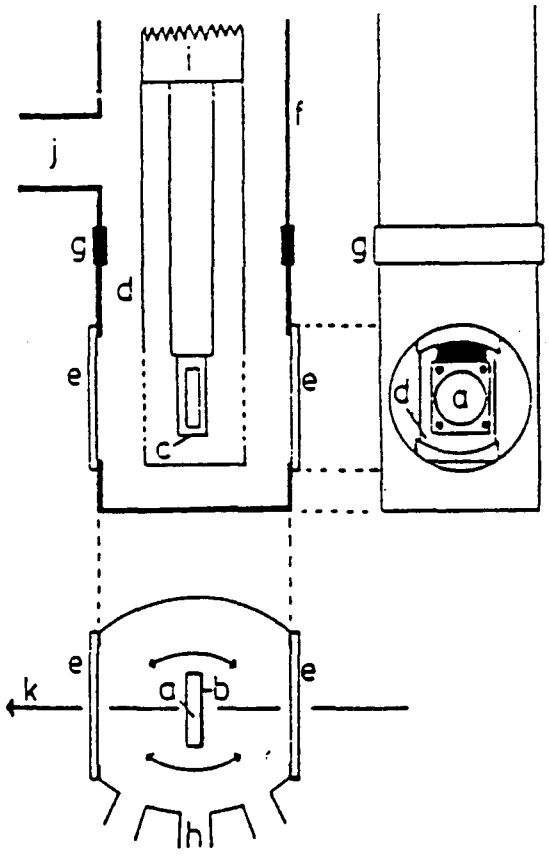

Fig.1-3. Schematic diagram of the sample area of equipment used for matrix isolation studies in the IR to UV region of the spectrum: (a) low temperature window; (b) matrix; (c) window holder; (d) radiation shield; (e) outer windows; (f) vacuum jacket; (g) rotatable seal allowing movement of central window relative to spray on spots; (h) spray or ports and holders of other equipment; (i) low temperature source; (j) pumping port; (k) path of IR or UV photolysis or detection beam.

A variation of the matrix isolation method is the use of glassy material , such as 1,2-epoxyethylbenzene, as a matrix at temperatures from 12K to 100K. A solution of a stable precursor may be made in a mixture of the solvent which usually has a high viscosity. This mixture is then frozen to a glass at low temperature between two CaF_2 windows in a suitable cell. Rapid freezing is required otherwise the solute simply crystallizes from solution. Once the glass has been successfully produced, however, the photochemical reactions of the trapped species may be followed as in the matrix isolation method.[15-18]. This technique has its limitations. Firstly, in these media the IR bands are usually not very sharp which reduces their value for structural characterization since overlapping features may easily be missed. Secondly, there is evidence that these glassy materials are not "inert" matrices and may interact in a significant way with the carbonyl fragment. There is however some evidence that the cage effect in these systems is a less serious problem than in matrices probably because of a less closely packed arrangement. In our case, we use 1,2-epoxyethylbenzene as the glassy material not only because this solvent forms a nice glass at low temperature, but also because it is transparent to a broad wavelength in the UV and visible region which allows one to do photochemistry with a broad band mercury lamp. Further more, this material stays as a glass at relatively high temperatures such as at 100K which allows us to study the subsequent thermal reaction of the photochemical intermediate with free CO.

The matrix isolation method has been used for many years to

study main group molecules and fragments with a small number of atoms, but studies of transition metal carbonyls and related species is a comparatively new field. It has proved to be a productive area with a rich variety of interesting structural results and a fascinating photochemistry. Indeed, photolysis of $Mo(CO)_6$ at 77K in methylcyclohexane glasses yields a long-lived intermediate that has been assigned as a coordinatively unsaturated species $Mo(CO)_5$ with C_{4v} symmetry. Infrared spectral changes observed at temperatures above 77K have been interpreted as the isomerization of the primary species with C_{4v} symmetry into one of D_{3h} symmetry[19-24].

1.4The geometry of unsaturated photochemical intermediates

Although the shapes of most saturated three-legged piano stool organometallic compounds are known, such as the 18 electron $CpMn(CO)_3$[25] as Y shaped, and the 16 electron complex $CpWR_2NO$[26] (R = alkyl) as T shaped, little is known about the shapes of three-legged piano stool unsaturated 16 electron intermediates resulting from the four-legged piano stool saturated 18 electron complexes.

The definition of the so-called T and Y shaped arrangement is somewhat ambiguous. Here is brief account of what is meant by T and Y shaped arrangement.

Four legged piano stool molecules which include dicarbonyl ligands can exist as cis or trans isomers (Fig.1-4).

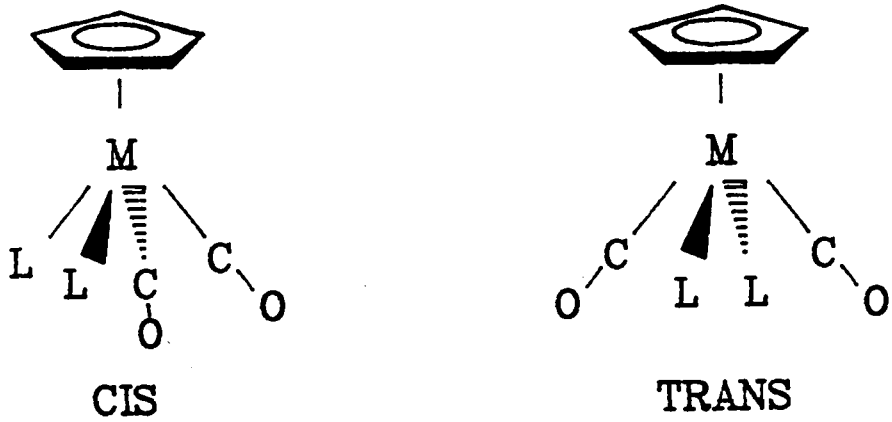

Fig.1-4: two isomers are possible for four-legged piano stool dicarbonyl molecules.

Fig.1-5 shows the stereochemical consequences of cis or trans isomers, including the two geometrical possibilities of intermediates, that is the so-called T and Y shaped ones. From Fig.1-5, we can clearly see that for T shaped intermediates, there are two distinct geometries resulting from cis and trans isomers. Each T shaped intermediate back reacts with the free CO to regenerate the starting compound. In other words, CO loss is from one position for both cis and trans isomers and the back reaction returns CO to that position. For Y shaped intermediates, however, it is unlikely that the cis and trans compounds will yield distinct CO loss product. This would result in facile isomerism from cis to trans or viceversa because it has three sites to which the free CO can coordinate. The T shaped intermediates which each have only one vacant coordination site may not undergo isomerization.

Previously, our group has studied both the isoelectronic series of compounds[27], $Cp^*Re(CO)_2X_2$, $Cp^* = \eta^5\text{-}C_5Me_5$, X = Me, Cl, Br, I, and the phosphine substituted molybdenum complexes[28] of the type $CpMo(CO)_2LX$, $Cp = \eta^5\text{-}C_5H_5$, L = CO, PPh_3, $P(nBu)_3$, X = Cl, Br, I. From our results, we've shown that the unsaturated Mo intermediate of the type CpMo(CO)LX is T shaped. This is confirmed since both the cis and trans $CpMoX(CO)_2LX$ upon photolysis lost CO, but each generated a different intermediate. The free CO generated above went back to the site where the loss of CO was occurring before during the thermal back reaction resulting in regeneration of the substrate (Fig.1-6). However, the geometry of the unsaturated 16 electron Rhenium intermediate of the type $Cp^*Re(CO)X_2$ remains unpredicted. Our results

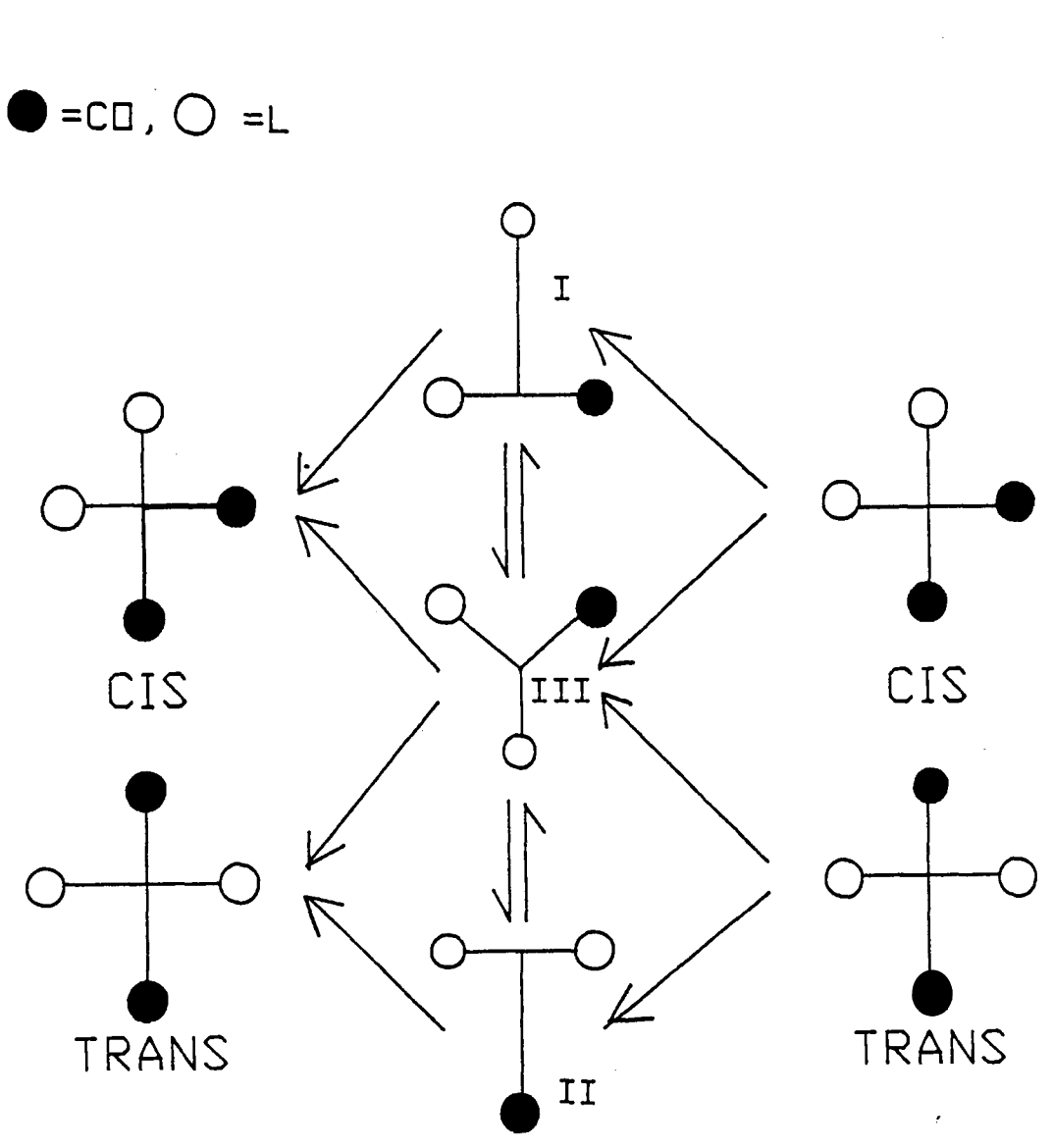

Fig.1-5: Stereochemical consequences of cis or trans isomers, including the possibility of rearrangement of intermediates. The Cp ring and metal are eliminated just for simplicity.

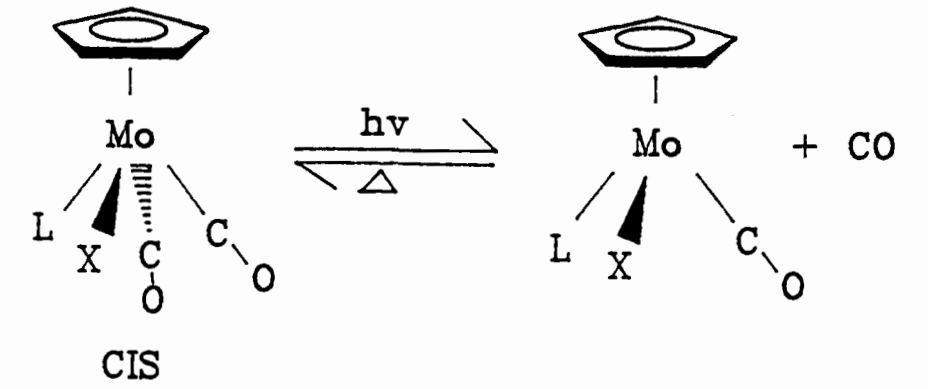

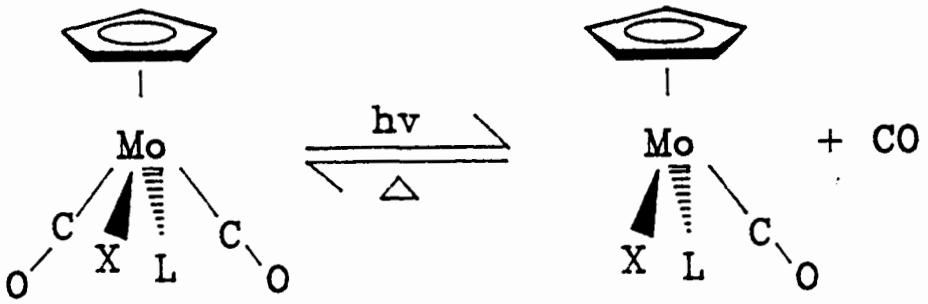

X = Cl, Br, I

L = CO, PPh_3, $P(nBu)_3$

Fig.1-6 The photochemistry of four-legged piano stool Mo complexes

show that both the cis and trans complex give the same intermediate upon photolysis which always yields the trans isomer during the thermal CO back reaction with the intermediate upon warming. This result is consistent with the intermediate being either T or Y shaped (Fig.1-7).

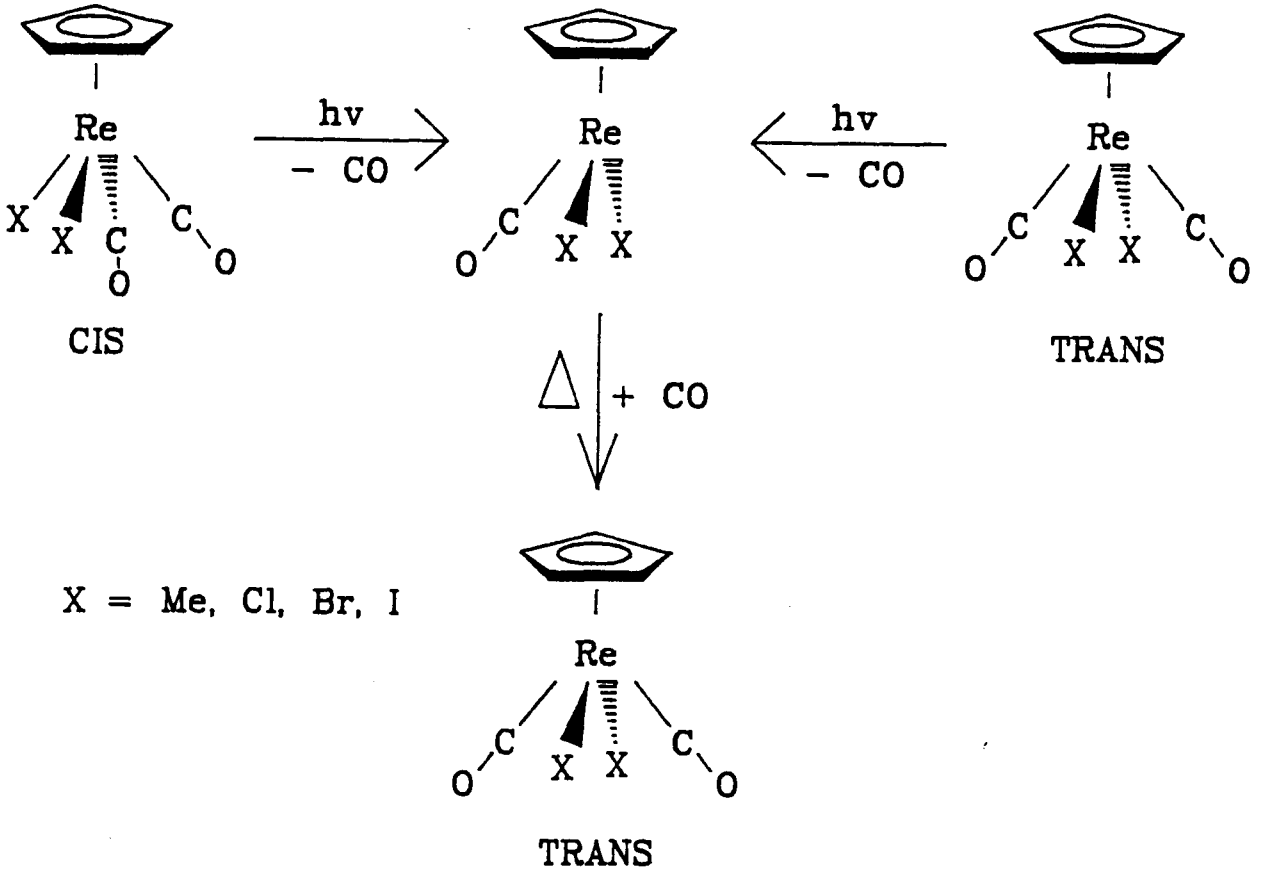

Fig.1-7 The photochemistry of four-legged piano stool Re complexes

1.5 Some theoretical methods for geometrical studies of photochemical intermediates

a. Force constants and Timney's method

The main tool used by our group to investigate photochemical intermediates is FTIR spectroscopy. The progress of the reaction is followed by observing of the disappearance of the metal carbonyl absorptions due to the starting material and the appearance of new peaks in the same region which correspond to the intermediate.

The most obvious features of metal carbonyl infrared spectra are the sharp, commonly intense absorptions in the 2150-1750 cm^{-1} region due to C-O stretching , ν(CO), vibrations. The analysis of these vibrations, to provide force constants, most frequently involves using the approximate Cotton-Kraihanzel force field (CKFF)[29-31]. This approximation is generally known as "energy factoring". Thus only two types of force constant are generated: (1) C-O stretching constants, K_{CO}; (2) CO-CO interaction constants, $K_{CO,CO}$.

Based on the CKFF approximation, Timney[32] proposed a simple empirical method for calculating the CKFF force constants and ultimately, for predicting νCO frequencies. The detail of this theory will be given in chapter 3. So, in practice, in order to determine the geometry of an intermediate, the carbonyl spectra of various compounds with known geometries are analyzed to get the ligand effect constants, then by using the force constants and ligand effect constants obtained before, the frequencies (or force constants) of various geometries of the intermediate are calculated and the one which gives best agreement between observed and calculated frequency (or force

constant) is probably the correct geometry.

b. EHMO method:

The so-called extended Huckel molecular orbital method, which was developed principally by Hoffmann[33], is a very powerful tool to explain the bonding, electron distribution, electronic energies, and conformational stabilities for transition metal molecules. A detailed account of this theory will be given in chapter 4.

The EHMO method, being an extension of the Huckel molecular orbital method, has several important advantages. First, because of its simplicity, it is easy to understand and apply, even to fairly complex systems. Second, it does not differ fundamentally from other more sophisticated and less inexact methods, and hence is very useful for developing a basic understanding of and feeling for quantum mechanical concepts, treatments, and results. Third, the results of this approximate theoretical treatment have contributed very significantly to both organic chemistry and inorganic chemistry since the 1960's. In our case, since we are studying the geometries of the photochemical intermediates, the use of the EHMO method is illuminating.

1.6 The research plan we set out to investigate

The study of four-legged piano stool molecules began with a low temperature photochemical investigation using FTIR spectroscopy.

By photolyzing the cis and trans compounds at low temperature, we were able to observe the intermediates resulting from the photoreaction. From the IR band positions and follow up thermal chemistry, we were able to judge whether we got different intermediates for both the cis and trans compounds or we got the same intermediates or more likely, a mixture of two different intermediates. The detailed results and discussions will be presented in the next chapter (chapter 2).

The IR study is followed by theoretical calculations using both Timney's method and the extended Huckel molecular orbital method. By using Timney's method, we were able to confirm the geometries which are proposed by the FTIR study by assuming that the one which gives the best agreement between observed and calculated frequencies is the right geometry. All these will be discussed in chapter 3.

In the calculations which involve the EHMO method, our goal was to calculate the energies of various geometrical possible conformations of our photochemical intermediates and then semiquantitatively determine the geometry of the intermediate. Also we hoped to explain the different geometries for the photochemical intermediates of different metal systems in terms of whether it is an electronic effect or simply a steric effect. The EHMO calculation will be presented in chapter 4. Chapter 5 is the experimental section.

Chapter 2: Photochemical studies on $CpM(CO)_2LX$

$M = V,\ L = X = PR_3,\ CO\ ;\ M = W,\ L = PR_3,\ X = Cl,\ I$

2.1 Introduction:

Previously, the low temperature photochemistry of both the isoelectronic series of compounds[27] $Cp^*Re(CO)_2X_2$ (X = Me, Cl, Br, I, $Cp^* = \eta^5\text{-}C_5Me_5$) and the phosphine substituted molybdenum complexes[28] of the type $CpMoX(CO)_2L$ ($Cp = \eta^5\text{-}C_5H_5$, X = Cl, Br, I, L = CO, PPh_3, $P(nBu)_3$), were investigated by FT-IR (fourier transform infrared spectroscopy).

In the Re case, it was found that photolysis of both the cis and the trans compound resulted in generation of a single CO loss product which always yielded the trans isomer during the CO back reaction with the unsaturated intermediate upon warming(eq.2-1).

$$cis\ or\ trans\text{-}CpRe(CO)_2X_2 \xrightarrow{h\nu} CpRe(CO)X_2 + CO \qquad (2\text{-}1)$$

$$CpRe(CO)X_2 \xrightarrow{\Delta} trans\text{-}CpRe(CO)_2X_2$$

For the Mo case, however, photolysis of both the cis and trans compounds resulted in the generation of distinct CO loss products, each of which reacted with CO to regenerate the starting complex in its original geometry(eq.2-2, 2-3).

$$cis\text{-}CpMo(CO)_2XL \underset{\Delta}{\overset{h\nu}{\rightleftharpoons}} CpMo(CO)XL + CO \qquad (2\text{-}2)$$

$$trans\text{-}CpMo(CO)_2XL \underset{\Delta}{\overset{h\nu}{\rightleftharpoons}} CpMo(CO)XL + CO \qquad (2\text{-}3)$$

The Re and Mo complexes above are all piano stool shaped molecules in which the four two electron ligands occupy the basal positions of the square pyramid and the center of mass of the cyclopentadienyl ligand occupies the apical position. Here, we extend this analysis to $CpM(CO)_2LX$, M = V, L = X = PR_3; M = W, L = PR_3, X = Cl ,I. We chose both the vanadium and the tungsten systems to investigate for the following reasons:

a. Four legged piano stool complexes also exist for both the Tungsten and Vanadium systems. Most of the known[34,35] compounds exhibit both cis and trans isomers which are stable. These complexes thus comprise a system ideally suited for investigating the stereochemistry of the photoisomerization process.

b. By studying these two systems, we will obtain results which we can compare with the other systems we previously studied, to see if they have the same reaction mechanism or if they react differently. This result will allow us to generalize reaction trends with respect to different metals and their corresponding ligands.

c. The low temperature study of the Mo and Re systems gave rise to an interesting point, i.e., the stereochemistry of the reaction

intermediate. Previous literature[36] on related trialkyl gold intermediates already showed that both T shaped and Y shaped geometries are possible for the intermediate and the energetics of the possible isomerizations between the two geometries. So we hoped to obtain more information on the geometry of the photochemical intermediates of both the Vanadium and Tungsten systems from this low temperature FTIR study.

2.2 The photochemistry of $CpV(CO)_{4-n}L_n$, n = 1,2.

Photolysis with broad band irradiation of $CpV(CO)_3P(OMe)_3$ in 1,2-epoxyethylbenzene at 12K results in loss of this complex. This has been shown by FTIR monitoring of the photolysis which indicates loss of intensity due to tricarbonyl compound at 1955, 1865, 1852 cm^{-1}, and the appearance of three new bands (Fig 2-1). The band at highest energy, 2130cm^{-1}, is assigned to free CO in the matrix[27]. The two remaining bands at 1925, 1822 cm^{-1} are due to the dicarbonyl complex $CpV(CO)_2P(OMe)_3$. The spectrum was obtained by subtracting the absorption spectra after photolysis from the one before photolysis. A negative peak indicates loss of intensity of that peak, while a positive one, appearance of a new peak. The relative intensity of the two bands associated with $CpV(CO)_2P(OMe)_3$ is 1:1.41 and the angle between the two CO ligands was calculated from $\tan^2\theta = Ia/Is$[37], as 109.5°. Here, 2θ is the angle between the two CO bonds. "Is" is the intensity of the symmetric CO stretching band which is at higher frequency and "Ia" is the intensity of the asymmetric CO stretching band

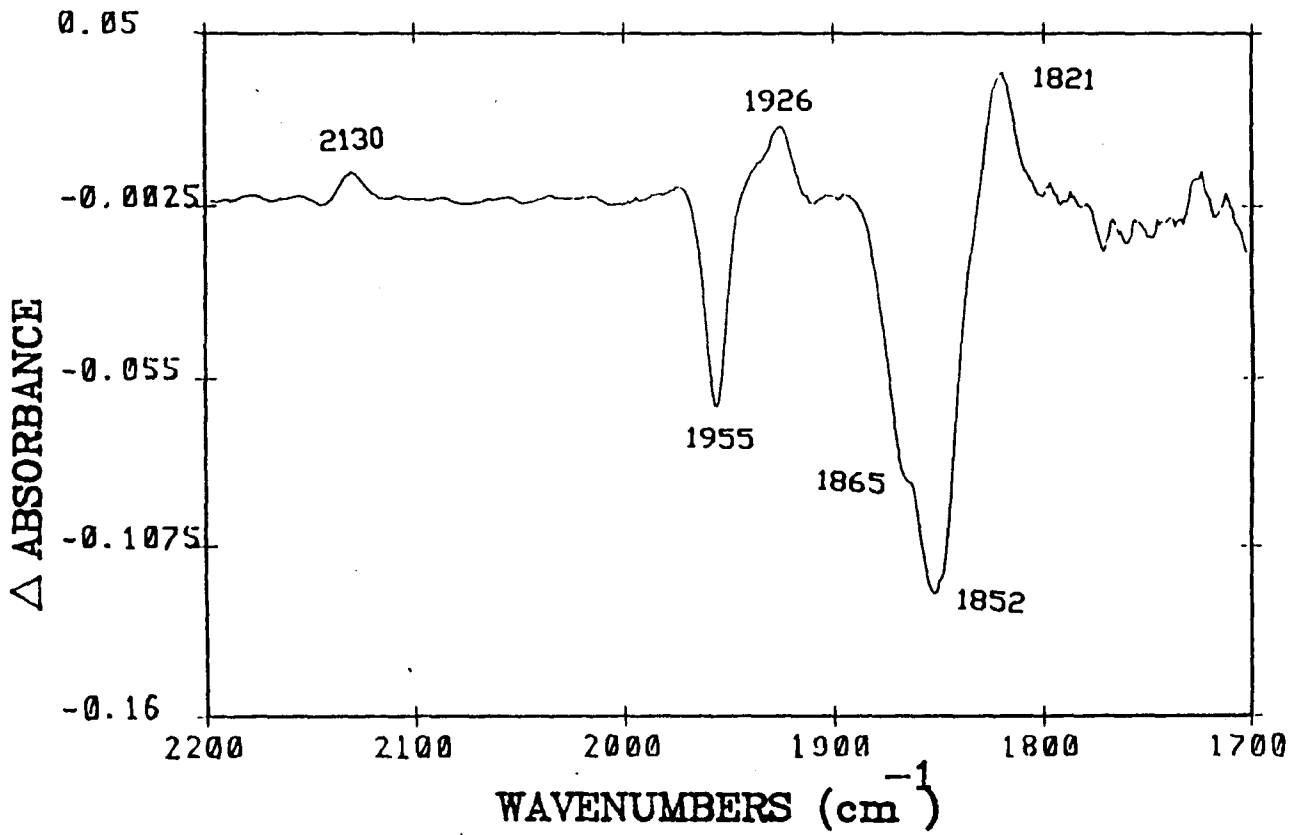

Fig. 2-1: FTIR spectral changes accompanying UV Photolysis of $CpV(CO)_3P(OMe)_3$ in 1,2-epoxyethylbenzene at 12K for 40 seconds

which is at lower frequency. This ratio indicates an approximate trans geometry for the remaining two ligands.

Surprisingly, besides the 16 electron unsaturated intermediate, we were also able to photodissociate a CO from the 16 electron intermediate to get a 14 electron unsaturated intermediate. This situation is very rare in organometallic photochemistry. All of the products were shown by FTIR monitoring of the reaction(Fig.2-2, 2-3). The two bands due to the 16 electron intermediate at 1926 and 1821 cm^{-1} ultimately disappeared and a new band at 1939 cm^{-1} appeared. This is assigned to the unsaturated 14 electron fragment $CpV(CO)P(OMe)_3$. A similar experiment was also conducted with $CpV(CO)_3P(OEt)_3$ in 1,2-epoxyethylbenzene at 12K. The results were essentially the same and the 14 electron fragment was also observed (see Table 2-1).

In addition to these absorptions, one band at 1726cm^{-1} is observed. This latter absorption is connected with the solvent being photolyzed. This is confirmed by photolyzing the deoxygenated solvent in the absence of any added compounds.

Photolysis of cis-$CpV(CO)_2[P(OMe)_3]_2$ in 1,2-epoxyethylbenzene at 12 K resulted in the loss of this complex. This was again shown by FTIR monitoring of the photolysis which indicates loss of intensity due to the dicarbonyl at 1871 and 1792 cm^{-1} and the appearance of the two new bands. The band at 2130cm^{-1} is assigned to free CO and the other one at 1815cm^{-1} is assigned to the unsaturated fragment $CpV(CO)[P(OMe)_3]_2$ (Fig.2-4).

Warming of the sample containing $CpV(CO)[P(OMe)_3]_2$ results in a reaction between the CO, generated above, and the monocarbonyl

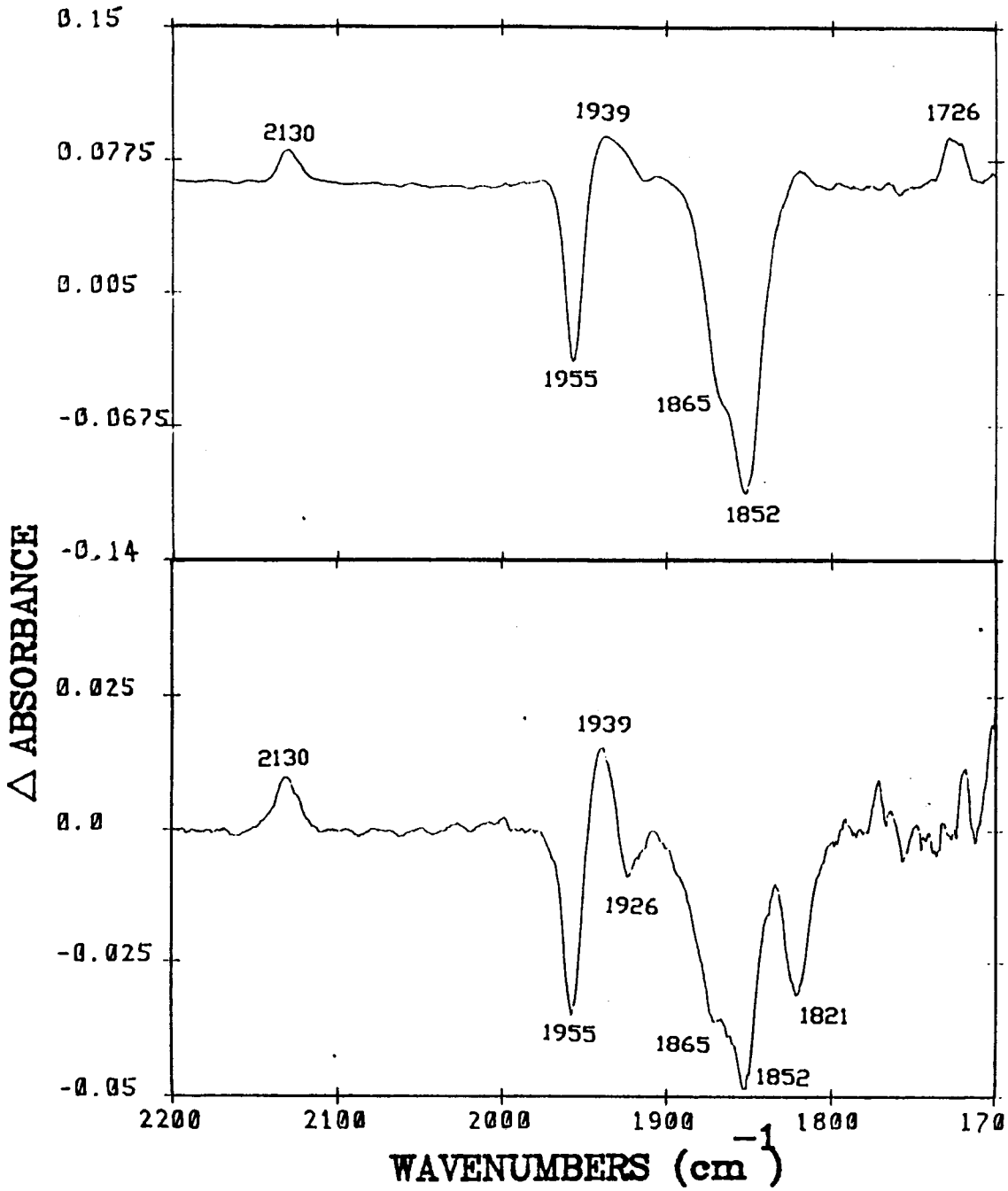

Above: Fig.2-2: FTIR spectral changes on further photolysis of $CpV(CO)_3P(OMe)_3$ in 1,2-epoxyethylbenzene at 12K for an additional 15 minutes

Below: Fig.2-3: The difference spectrum between the two spectra in Fig.2-1 and Fig.2-2

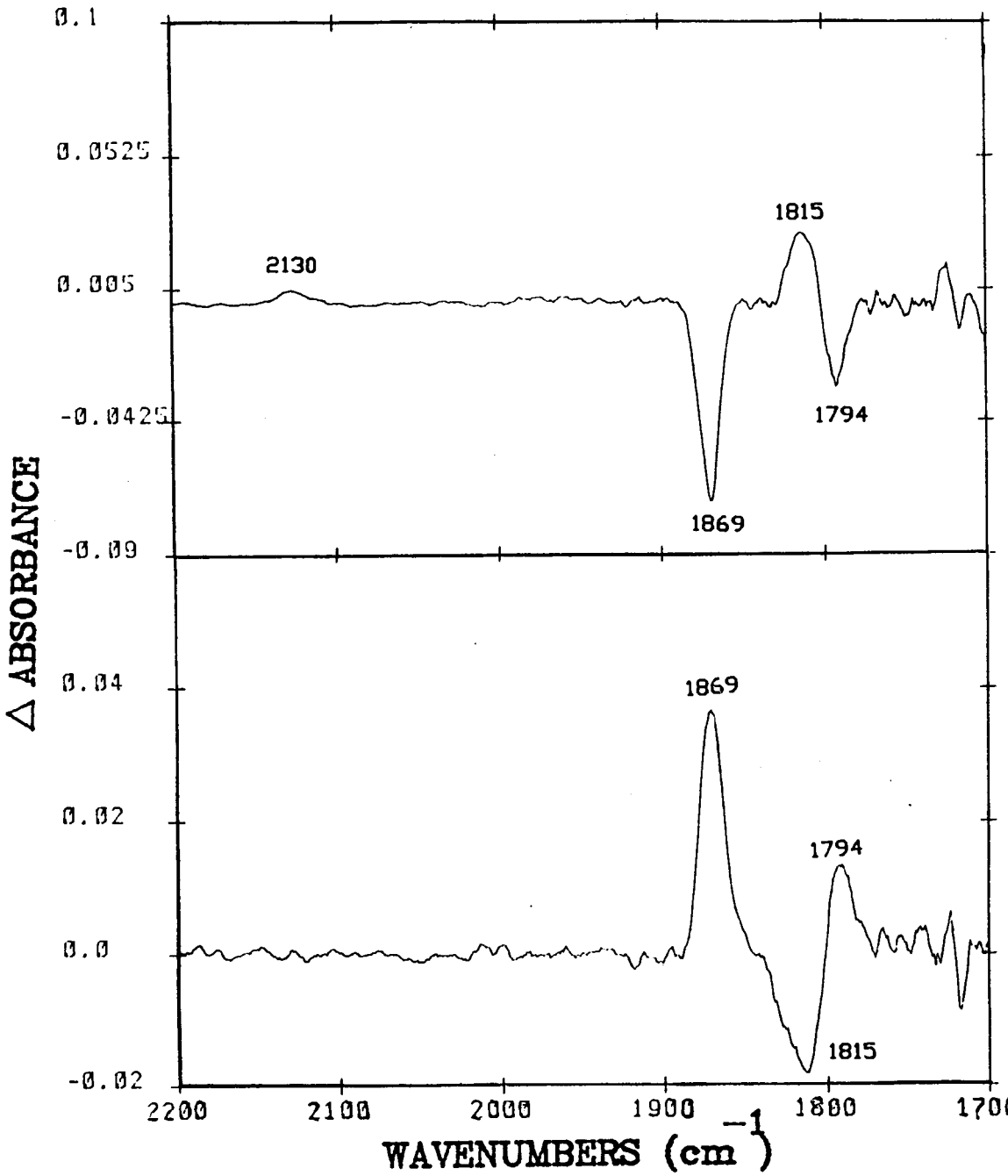

Above: Fig.2-4: FTIR spectral changes accompanying UV photolysis of cis-$CpV(CO)_2[(POMe)_3]_2$ in 1,2-epoxylethylbenzene at 12K for 1 minute

Below: Fig.2-5: FTIR spectral changes associated with warming photoproduced $CpV(CO)[P(OMe)_3]_2$ and CO from 12K to 100K

fragment. The product of this reaction is identified by FTIR to be the starting complex cis-$CpV(CO)_2[P(OMe)_3]_2$ (Fig.2-5).

Similar experiments were conducted with cis-$CpV(CO)_2[P(OEt)_3]_2$. The result in this case was in qualitative agreement with the results for cis-$CpV(CO)_2[P(OMe)_3]_2$. In each case, CO was lost and an unsaturated monocarbonyl complex was formed. On warming, the starting complex was regenerated. The spectral changes are summarized in Table 2-1.

The FTIR monitored photolysis of trans-$CpV(CO)_2[P(OMe)_3]_2$ in 1,2-epoxyethylbenzene at 12K leads to loss of intensity of two bands at 1883 and 1791 cm^{-1} due to the starting complex, and appearance of two new bands at 2130 and 1729 cm^{-1}. One of these new bands is of course the band of the free CO in the matrix, and the other one is assigned to the monocarbonyl complex $CpV(CO)[P(OMe)_3]_2$. Although the latter band is so close to the band of the solvent being photolyzed (1726 cm^{-1}), it is confirmed to be the intermediate band since the band appeared in less than 2 minutes of photolysis while the production of the solvent band needs at least ten minutes of photolysis. On warming, the unsaturated intermediate reacted with CO to regenerate the starting complex once again in its original geometry, however, nothing happened to the solvent band. this is again an indication that the band at 1729 cm^{-1} is indeed due to the intermediate.

The above experiments were repeated with trans-$CpV(CO)_2[P(OEt)_3]_2$, the result obtained was analogous to the results described above. The FTIR data for the complex and its CO loss products are summarized in Table 2-1.

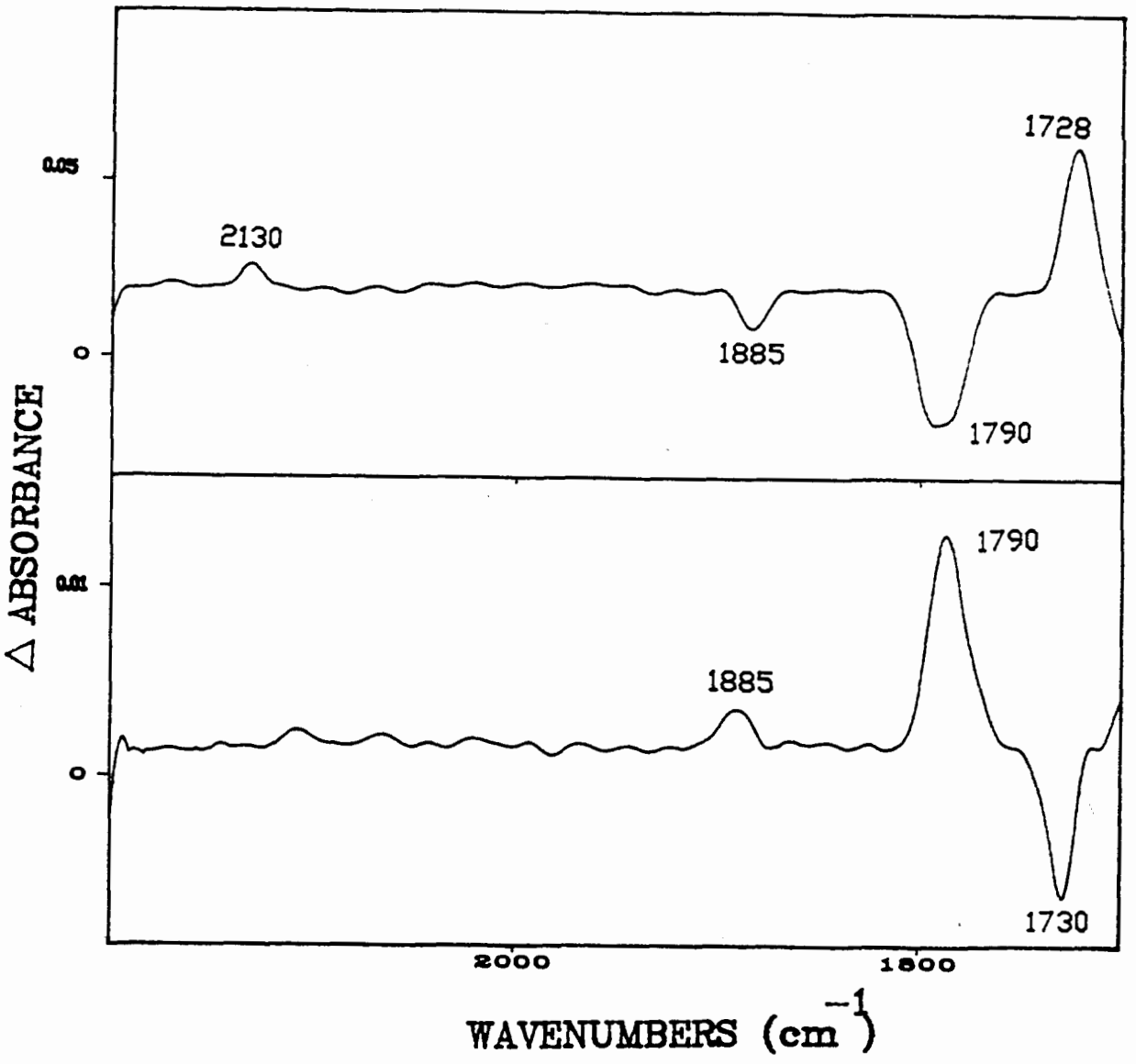

Above: Fig.2-6: FTIR spectral changes accompanying UV photolysis of trans-$CpV(CO)_2[P(OEt)_3]_2$ in 1,2-epoxyethylbenzene at 77K for 2 hours, the peak at 1728 cm^{-1} is due to the degeneracy of the intermediate peak at 1730 cm^{-1} and the solvent peak at 1726 cm^{-1}.

Below: Fig.2-7: FTIR spectral changes associated with warming photoproduced $CpV(CO)[P(OEt)_3]_2$ and CO from 12K to 100K

Table 2-1: FTIR SPECTRA OF RELEVANT VANADIUM COMPOUNDS

Complex	ν(CO) (cm^{-1})[a]
$CpV(CO)_3P(OMe)_3$	b.1957(1.0)[d], 1865(1.3), 1852(1.8)
$CpV(CO)_2P(OMe)_3$	b.1926(1.0), 1821(1.4)
$CpV(CO)P(OMe)_3$	b.1939
$CpV(CO)_3P(OEt)_3$	b.1955(1.0), 1864(1.1), 1848(1.6)
$CpV(CO)_2P(OEt)_3$	b.1923(1.0), 1818(2.4)
$CpV(CO)P(OEt)_3$	b.1936
cis-$CpV(CO)_2[P(OMe)_3]_2$	b.1871(2.1), 1794(1.0)
cis-$CpV(CO)[P(OMe)_3]_2$	b.1815
trans-$CpV(CO)_2[P(OMe)_3]_2$	b.1883(1.0), 1791(4.6) c.1886(1.0), 1790(4.3)
trans-$cpV(CO)[P(OMe)_3]_2$	b.1729 c.1730
cis-$CpV(CO)_2[P(OEt)_3]_2$	c.1863(1.8), 1785(1.0)
cis-$CpV(CO)[P(OEt)_3]_2$	c.1807
trans-$CpV(CO)_2[P(OEt)_3]_2$	b.1883(1.0), 1790(5.0) c.1885(1.0), 1790(4.7)
trans-$cpV(CO)[P(OEt)_3]_2$	b.1728 c.1730

a. All data were recorded in a 1,2-epoxyethylbenzene glass
b. FTIR data recorded at 12K
c. FTIR data recorded at 77K
d. The numbers in the brackets are the relative intensities of the IR bands

Some of the experiments were conducted again at 77K with similar results. These are also summarized in Table 2-1. The temperature change did not affect the reaction mechanism nor did it change the geometry of the intermediate. Fig.2-6 and 2-7 shows the photochemical behaviour of trans-$CpV(CO)_2[P(OEt)_3]_2$ at 77K.

2.3 The photochemistry of $CpW(CO)_{3-n}L_nX$, n = 0, 1

a. At 12K:

Photolysis of cis-$CpW(CO)_2[P(nBu)_3]I$ at 12K leads to the changes in the FTIR spectra as shown in Fig.2-8. Loss of FTIR absorptions due to the starting complex at 1933 and 1841cm^{-1} occur upon photolysis. The production of two new absorptions at 2130,and 1782 cm^{-1} is observed and found to occur proportionately to the loss of intensity associated with cis-$CpW(CO)_2[P(nBu)_3]I$. The absorption at 2130cm^{-1} is due to the production of free CO in the glass. The other absorption is logically due to the CO loss product $CpW(CO)[P(nBu)_3]I$. This assignment is consistent with the observed single absorption band, as expected for a monocarbonyl complex, and also with the subsequent reactivity associated with this species.

Upon warming the glass containing $CpW(CO)[P(nBu)_3]I$, absorptions due to CO and monocarbonyl fragment disappeared, and peaks at 1933 and 1841cm^{-1} appeared, this is the starting compound, cis-$Cp(CO)_2[P(nBu)]_3I$, and is the only observable product (Fig.2-9).

The above experiment was repeated with L=PPh_3, $P(OMe)_3$ and the

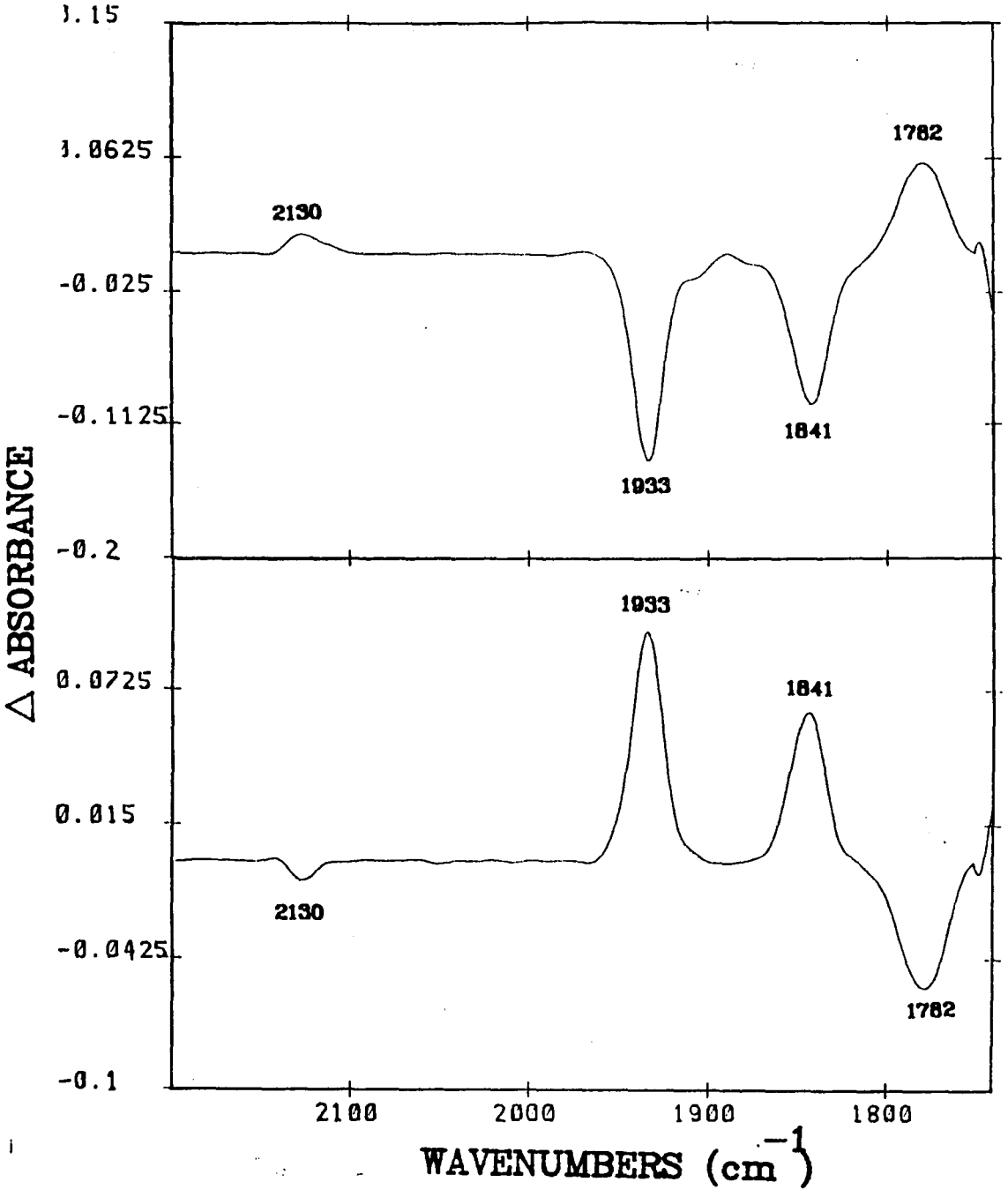

Above: Fig.2-8: FTIR spectral changes accompanying UV photolysis of cis-$CpW(CO)_2[P(nBu)_3]I$ in 1,2-epoxyethylbenzene at 12K

Below: Fig.2-9: FTIR spectral changes associated with warming photoproduced $CpW(CO)[P(nBu)_3]I$ and CO from 12K to 100K

results were essentially the same. In each case, the starting complex was lost and a monocarbonyl complex was formed during photolysis. On warming, cis-$CpW(CO)_2LI$ was regenerated. The spectral data for these compounds and their unsaturated species are summarized in Table 2-2.

A similar photolysis of the trans isomer was conducted. Once again, CO was lost to produce the unsaturated species. This was again shown by FTIR. The two bands due to trans-$CpW(CO)_2[P(nBu)_3]I$ at 1936 and 1848cm^{-1} were lost upon photolysis and the monocarbonyl fragment at 1798cm^{-1} was obtained. This intermediate was different from the one resulting from photolysis of the cis isomer. This was indicated by the different FTIR absorption bands for the two intermediates. The intermediates obtained from photolyzing the cis and trans isomers differed by 7cm^{-1} in ν(CO), and their subsequent reaction chemistry with free CO was also different.

On warming, the monocarbonyl fragment reacted with CO produced during photolysis to regenerate the starting complex, trans-$CpW(CO)_2[P(nBu)_3]I$. There was no cis isomer formed during the CO thermal back reaction. This result was confirmed by the fact that both the IR band positions and the integrated ratio of the two bands before and after photolysis (followed by subsequent warming up) are consistent. This was an indication of only the trans isomer. If there was any of the cis isomer produced, the IR bands would shift, and also the intensity ratio between the two IR bands would change.

The above sequence of experiments was conducted for the other complexes, trans-$CpW(CO)_2LI$, L= PPh_3, $P(OMe)_3$. The results were qualitatively the same. FTIR absorption bands for these complexes

are given in Table 2-2. In Fig.2-10 and Fig.2-11 is shown the spectral changes for trans-$CpW(CO)_2[P(nBu)_3]_2$. Irradiation at 12K resulted in the loss of CO from the coordination sphere and the production of $CpW(CO)IL$, L=PPh_3, $P(OMe)_3$. When the resultant glass was warmed , bands due to the unsaturated species and free CO were lost and those due to trans-$CpW(CO)_2LI$ were produced.

b.At 77k

The photochemical results at 12K suggest that both cis and trans compounds form independent intermediates with rigid geometry, but early reports on the photochemistry of compounds $CpM(CO)_3X$[38] in the presence of an additional ligand L (M=Mo, X=Br, I; M=W, X=Cl, Br, I, L = Phosphines) indicates that facile isomerism is also possible for the intermediate prior to the capture of the entering ligands. So, by conducting the experiments at a higher temperature, the barrier for the isomerization may be overcome. We then conducted the following experiments at the relatively high temperature of 77K.

Irradiation of 1,2-epoxyethylbenzene solutions of $CpW(CO)_3I$ at 77K leads to loss of FTIR absorptions due to the starting complex at 2032,1930 cm^{-1} and the production of cis-$CpW(CO)_2I$, as evidenced by FTIR absorptions at 1988,1846cm^{-1}, the cis geometry was indicated by the angle between the two CO ligands, 74.8°, which was calculated using the intensity ratio of the resulting two bands. This was consistent with early reports on the photoreaction of $CpW(CO)_3I$ with addition of PPh_3, only cis-$CpW(CO)_2PPh_3I$ is formed.

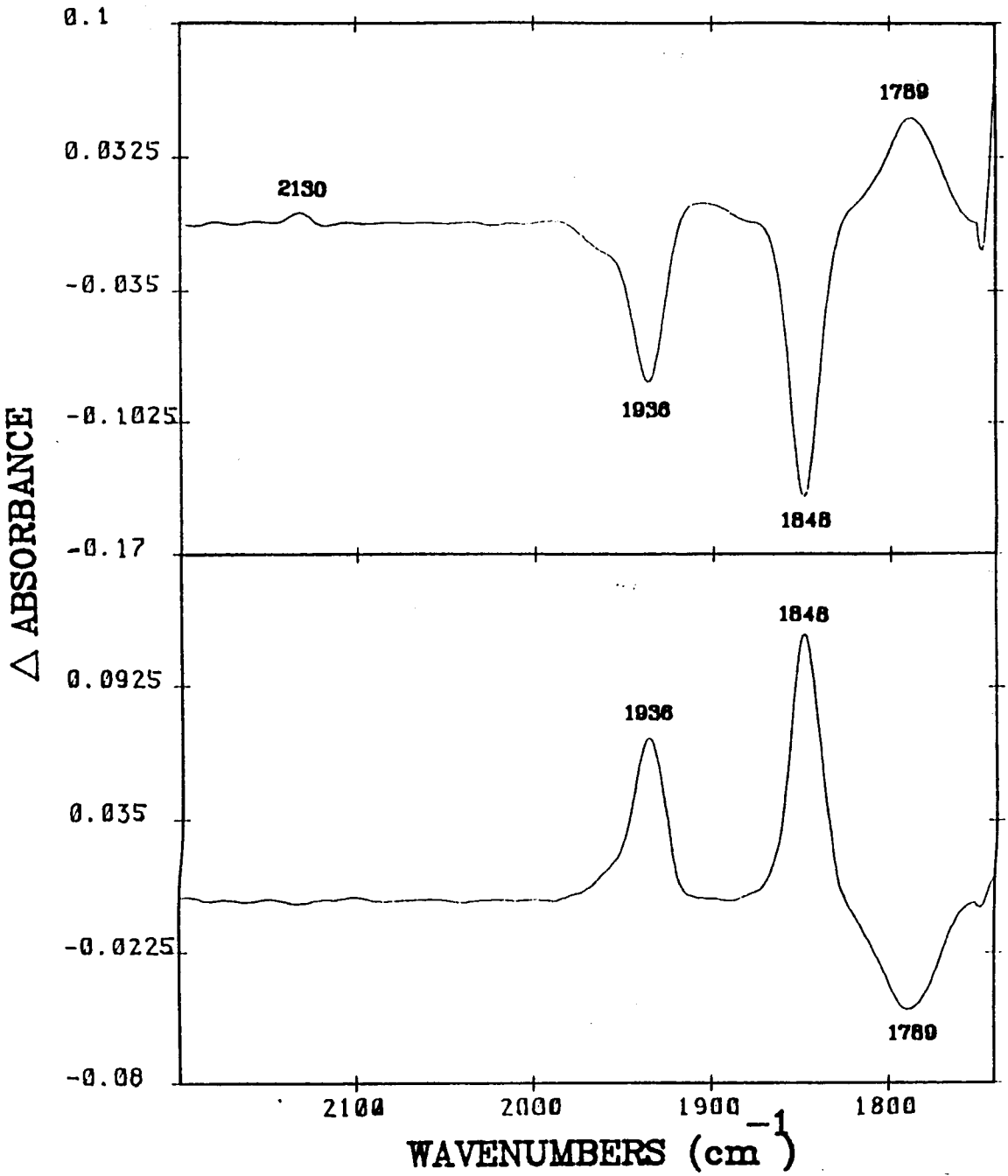

Above: Fig.2-10: FTIR spectral changes accompanying UV photolysis of trans-$CpW(CO)_2[P(nBu)_3]I$ in 1,2-epoxyethylbenzene at12K

Below: Fig.2-11: FTIR spectral changes associated with warming photoproduced $CpW(CO)[P(nBu)_3]I$ and CO from 12K to 100K

Table 2-2: FTIR SPECTRA OF RELEVANT TUNGSTEN COMPOUNDS AT 12K

Complex	ν(CO) (cm^{-1})[a]
cis-$CpW(CO)_2PPh_3I$	1940(1.5)[c], 1854(1.0)
cis-$CpW(CO)\bar{P}Ph_3\bar{I}$	1794
trans-$CpW(CO)_2PPh_3I$	1949(1.0), 1861(2.9)
trans-$CpW(CO)\bar{P}Ph_3\bar{I}$	1808
cis-$CpW(CO)_2P(nBu)_3I$	1933(1.5), 1841(1.0)
cis-$CpW(CO)\bar{P}(nBu)_3\bar{I}$	1782
trans-$CpW(CO)_2P(nBu)_3I$	1936(1.0), 184891.7)
trans-$CpW(CO)\bar{P}(nBu)_3\bar{I}$	1789
cis-$CpW(CO)_2P(OMe)_3I$[b]	1952(1.2), 1874(1.0)
cis-$CpW(CO)\bar{P}(OMe)_3\bar{I}$	1822
trans-$CpW(CO)_2P(OMe)_3I$	1959(1.0), 1877(2.3)
trans-$CpW(CO)\bar{P}(OMe)_3\bar{I}$	1824.6

a. All data recorded of glass at 12K, the solvent is 1,2-epoxyethylbenzene
b. The cis-$CpW(CO)_2P(OMe)_3I$ has some trans isomer in it, which in turn produces the trans intermediate and hence, the trans isomer upon warming
c. numbers in brackets are the relative intensities of the IR bands

Similar results were obtained with $CpW(CO)_3Cl$, again, the cis unsaturated dicarbonyl intermediate was the only product (Table 2-3). The intermediate was still stereochemically rigid as evidenced by the fact that only one intermediate with specific geometry is produced during the photolysis.

Photolysis of cis-$CpW(CO)_2[P(nBu)_3]I$ in the same solvent at 77K results in the production of two new bands at 2130 and 1784cm^{-1} at the expense of the starting material at 1932 and 1839cm^{-1}. The band at 2130cm^{-1} is again due to the free CO in the matrix and the other band at 1784cm^{-1} is reasonably due to the CO loss product $CpW(CO)P(nBu)_3I$. Notably, this band is between the band at 1782cm^{-1}, which is produced by photolysis of cis-$CpW(CO)_2[P(nBu)_3]I$ at 12K, and the band at 1789cm^{-1}, which is produced by the trans isomer during photolysis at 12K (Fig.2-12).

However, the subsequent reactivity was very much different from similar process starting at 12K. On warming the glass containing the monocarbonyl and free CO, two bands at 1934 and 1847 cm^{-1} were produced while the monocarbonyl complex and free CO decreased in intensity. These two band positions differed significantly from the starting complex, especially, the symmetric band. In this case, ν(CO) shifted by 8cm^{-1}. Evidently, not all the intermediate converted back to the starting complex, cis-$CpW(CO)_2P(nBu)_3I$, some trans isomer must be produced (Fig.2-13). The relative intensity between the two resulting bands is 1.12:1 (compare with 1.50:1 before photolysis).

Similar experiments were conducted with the trans isomer under identical conditions. Again the starting complex was lost upon

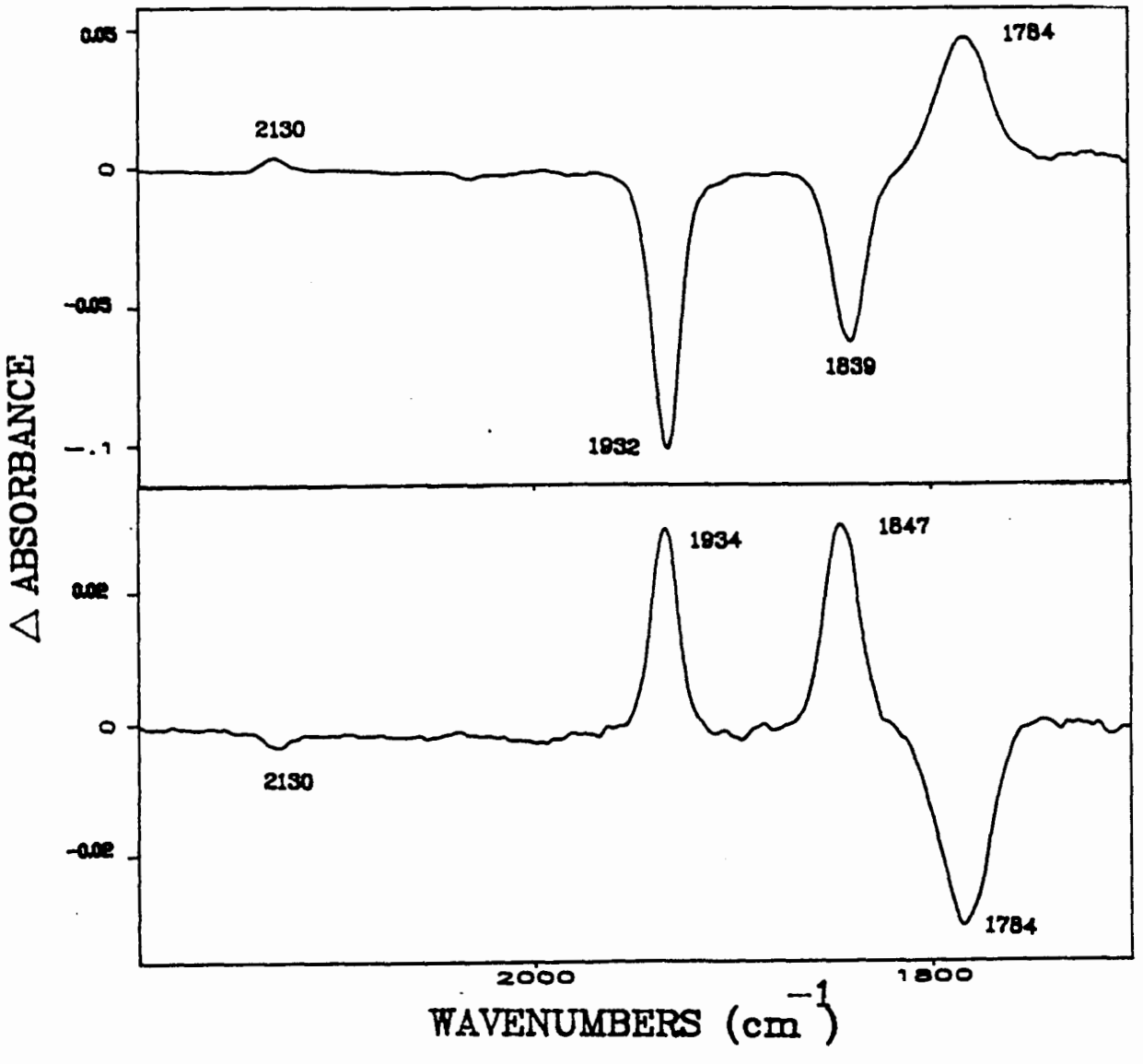

Above: Fig.2-12: FTIR spectral changes accompanying UV photolysis of cis-$CpW(CO)_2[P(nBu)_3]I$ in 1,2-epoxyethylbenzene at 77K

Below: Fig.2-13: FTIR spectral changes associated with warming photoproduced $CpW(CO)[P(nBu)_3]I$ and CO from 77K to 100K

photolysis, which was shown by FTIR absorption at 1935 and 1849cm^{-1} and the production of two bands, one at 2130cm^{-1} was the free CO, and the other one at 1784cm^{-1} was the same as the intermediate which was produced from photolyzing the cis isomer. This suggests the resultant glass contains a mixture of intermediates with cis and trans geometry (Fig.2-14).

On warming, the glass containing the intermediate and free CO, two bands at 1934 and 1847cm^{-1} were produced (Fig.2-15). The integrated ratio between the resulting two bands was calculated as 1.13:1 (compare with 1:1.28 before photolysis) which was consistent with the behaviour of a mixture of intermediates produced by the cis isomer. So this photolyzed glass must again contain a mixture of both the cis and trans intermediates since it behaves the same as the one produced by the cis isomer. Due to the degeneracy of the IR bands of the cis and trans product on warming, the relative yield of the cis and trans isomers obtained upon warming was not calculated. From the ratio of the two resulting bands upon warming, we predict that more cis isomer was produced than the trans isomer. A non-selective reaction would produce a ratio of 2:1 ,cis to trans[39].

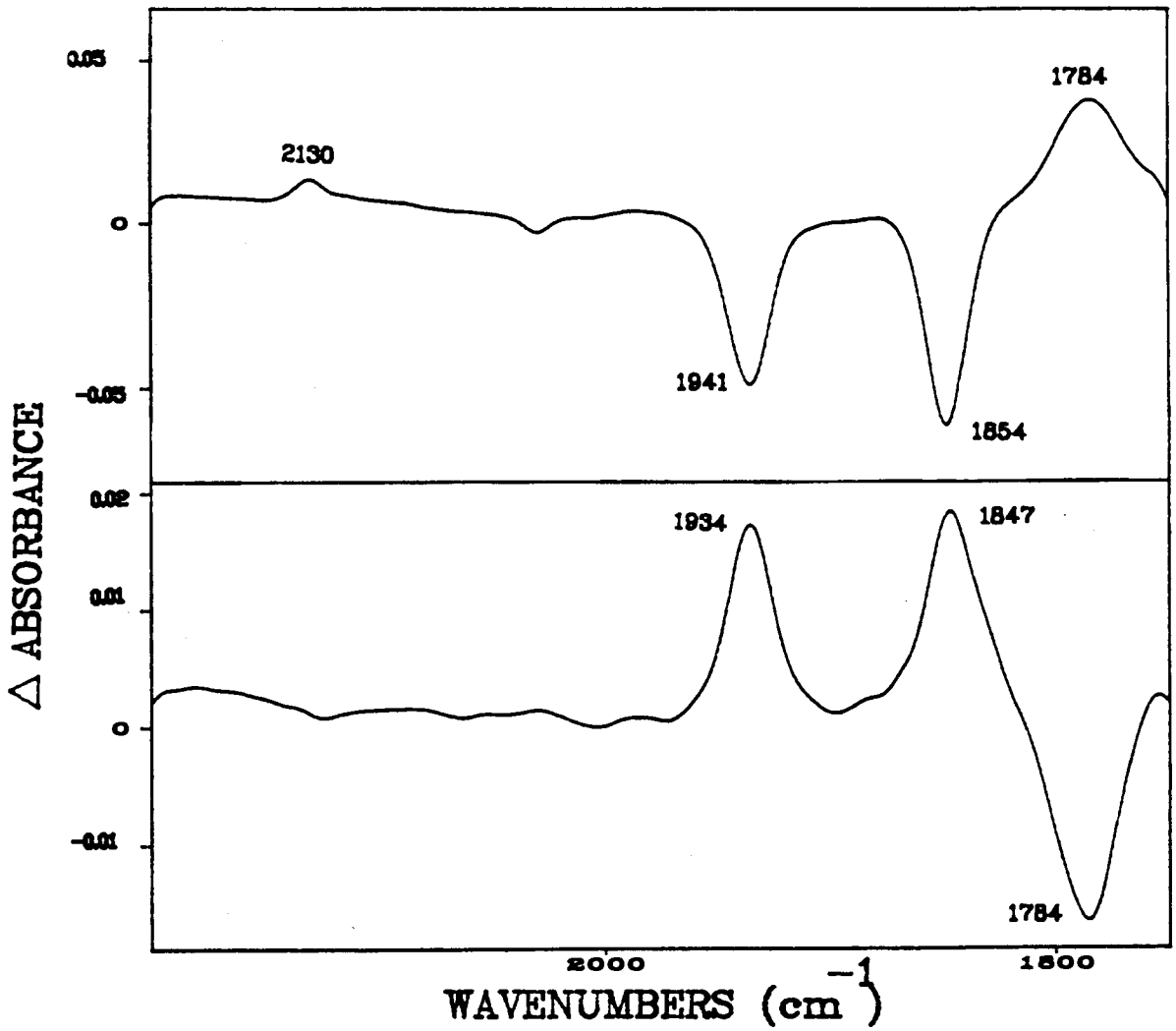

Above: Fig2-14: FTIR spectral changes accompanying UV photolysis of trans-$CpW(CO)_2[P(nBu)_3]I$ in 1,2-epoxyethylbenzene at77K

Below: Fig.2-15: FTIR spectral changes associated with warming photoproduced $CpW(CO)[P(nBu)_3]I$ and CO from 77K to 100K

Table 2-3: FTIR SPECTRA OF RELATED TUNGSTEN COMPLEXES AT 77K

COMPOUND	ν(CO) (cm^{-1})[a]
$CpW(CO)_3I$	2031(1.0)[b], 1933(1.4)
cis-$CpW(CO)_2I$	1988(1.2), 1846(1.0)
cis-$CpW(CO)_2P(nBu)_3I$	1931.5(1.7), 1839(1.0)
cis-$CpW(CO)P(nBu)_3I$	1784
trans-$CpW(CO)_2P(nBu)_3I$	1935.4(1.0), 1848.6(1.3)
trans-$CpW(CO)P(nBu)_3I$	1784
cis-$CpW(CO)_2PPh_3I$	1941.2(1.7), 1854.4(1.0)
cis-$CpW(CO)PPh_3I$	1796
trans-$CpW(CO)_2PPh_3I$	1950.8(1.0), 1864(3.2)
trans-$CpW(CO)PPh_3I$	1796
cis-$CpW(CO)_2P(OMe)_3I$	1950(1.5), 1869(1.0)
cis-$CpW(CO)P(OMe)_3I$	1822
trans-$CpW(CO)_2P(OMe)_3I$	1961.4(1.0), 1876.6(3.7)
trans-$CpW(CO)P(OMe)_3I$	1826
$CpW(CO)_3Cl$	2041(1.0), 1951(1.1), 1936(1.3)
cis-$CpW(CO)_2Cl$	1981(1.4), 1837(1.0)
cis-$CpW(CO)_2P(OMe)_3Cl$	1955.7(1.8), 1867.9(1.0)
cis-$CpW(CO)P(OMe)_3Cl$	1815.8
cis-$CpW(CO)_2PPh_3Cl$	1944(1.7), 1854(1.0)
cis-$CpW(CO)PPh_3Cl$	1796.5

a. All data recorded at 77K in 1,2-epoxyethylbenzene glass.
b. numbers in brackets are the relative intensities of the IR bands

2.4 Discussion:

a. Vanadium complexes:

The photo lability of $CpV(CO)_4$ has been employed in preparing a variety of $CpV(CO)_{4-n}L_n$ complexes by irradiating $CpV(CO)_4$ in the presence of L[2-5]. Previous literature shows that the CO ligand in $CpV(CO)_3PPh_3$ is not photo sensitive[6] and loss of PPh_3 is the preferential step for the excited-state $CpV(CO)_3PPh_3$ decay. This is confirmed by photolyzing $CpV(CO)_3PPh_3$ in CO saturated benzene and observing the rapid appearance of $CpV(CO)_4$. Our results at 12K show that both phosphine substituted dicarbonyl complex or tricarbonyl complex are photosensitive and CO loss is the only observable process under our conditions. For the tricarbonyl complex, loss of a second CO is also possible (eq.2-4, 2-5).

$$CpV(CO)_3L \xrightarrow{h\nu} CpV(CO)_2L + CO \qquad (2\text{-}4)$$

$$CpV(CO)_2L \xrightarrow{h\nu} CpV(CO)L + CO \qquad (2\text{-}5)$$

Irradiation of $CpV(CO)_4$[40] with high-energy radiation (UV) in Ar and CH_4[12] matrices primarily resulted in ejection of CO ligands and the formation of $CpV(CO)_n$ (n=1-3) where n has been established by ^{13}CO labelling. Molecular orbital calculations[41] have shown that two geometries are possible for the coordinatively unsaturated fragment $CpV(CO)_2$ as so called cis and trans geometry (some call them as pyramidal and planar). So, if we substitute one empty position in

$CpV(CO)_2$ with one phosphine, both the cis and trans geometry should still be possible (Fig.2-16).

In the case of 16 electron species $CpMn(CO)_2$, the pyramidal geometry was preferred over a planar geometry[42]. For a consideration of OC-M-CO (θ) bond angles in the first-row transition metal $CpM(CO)_2$ species, M=Co, 18-electron complex, θ=96°,(solution)[43] and θ=94° (CO matrix)[44], M=Mn, 16-electron complex, θ=99 and 101° (Ar and CH_4 matrix)[45], the OC-V-CO angle of 77° and 114° was calculated for the

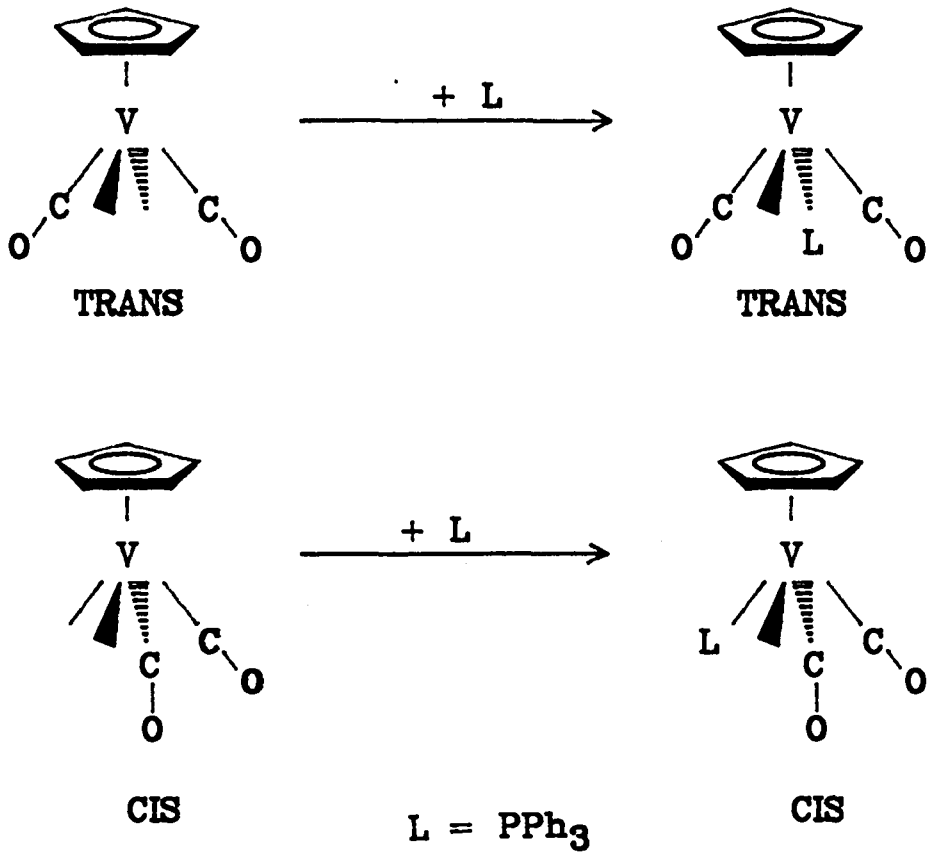

Fig.2-16: Two geometries are possible for coordinativly unsaturated complex $CpV(CO)_2$ as well as $CpV(CO)_2PPh_3$

cis and trans fragment[40]. Our experimental result of the OC-V-CO angle 109.5° for $CpV(CO)_2PPh_3$ indicates the trans geometry is preferred over the cis one. So for the second CO loss product, the geometry with one CO and a phosphine ligand cis to each other is expected.

The observation of only trans-$CpV(CO)_2PPh_3$ upon photolysis of $CpV(CO)_3PPh_3$ indicates that the intermediate is a T shaped one. This T shaped geometry is further indicated by the observation that the cis and trans-$CpV(CO)_2L_2$ molecules give rise to discreet CO loss products. Both intermediates have different spectroscopic properties (IR band position)and the subsequent reactivity toward CO are also different. Each unsaturated isomer reacts with CO to generate a specific geometry of the dicarbonyl complexes (starting complexes). These complexes must be stereo-isomers. This is again an indication of T shaped intermediates. The intermediate must be stereochemically rigid since in each case CO is lost and a specific intermediate is produced. This CO returns to the position from where it was lost to result in regeneration of the starting material with its original geometry.

Kinetic studies of the thermal substitution reactions of $CpV(CO)_4$ with a variety of phosphines and phosphites have suggested that the reaction proceeds by dissociative paths in which loss of a CO ligand is the rate determining step[6]. However, some have argued for an associative pathway for the photochemical reaction of $CpV(CO)_4$ with PPh_3[46] according to the quantum yield data. Our results show clearly that CO loss is the preferential step for the excited-state $CpV(CO)_{4-n}L_n$ (n = 1, 2) decay. This confirms the dissociative

pathway. In other words, the sterically crowded 20 electron $CpV(CO)_{4-n}L_nL'$ (L′ is the entering ligands, n= 1, 2) is unlikely in this case.

b. Tungsten complexes:

Previous reports on $CpW(CO)_3X$ and related complexes suggest a variety of possible reaction routes for excited-state $CpW(CO)_3X$ complexes. They include carbon monoxide dissociation (eq.2-6), heterolytic cleavage of the metal-halogen bond (eq.2-7) and homolytic cleavage of the metal-halogen bond (eq.2-8).

$$CpW(CO)_3X \xrightarrow{h\nu} CpW(CO)_2X + CO \qquad (2\text{-}6)$$

$$CpW(CO)_3X \xrightarrow{h\nu} CpW(CO)_3^{+} + X^{-} \qquad (2\text{-}7)$$

$$CpW(CO)_3X \xrightarrow{h\nu} CpW(CO)_3^{\cdot} + X^{\cdot} \qquad (2\text{-}8)$$

For phosphines or phosphites substituted tungsten dicarbonyl derivatives, $CpW(CO)_2LX$, dissociation of the phosphine ligand (eq.2-9) and geometric isomerization (eq.2-10 and eq.2-11) are also possible processes for excited-state decay.

$$CpW(CO)_2LX \xrightarrow{h\nu} CpW(CO)_2X + L \qquad (2\text{-}9)$$

$$\textit{cis}\text{-}CpW(CO)_2LX \xrightarrow{h\nu} \textit{trans}\text{-}CpW(CO)_2LX \qquad (2\text{-}10)$$

$$\textit{trans}\text{-}CPW(CO)_2LX \xrightarrow{h\nu} \textit{cis}\text{-}CpW(CO)_2LX \qquad (2\text{-}11)$$

All the above results are however obtained at room temperature. Our results indicate that CO loss is the only observable process upon photolysis of $CpW(CO)_2LX$ at temperatures below 77k (eq.2-12).

$$CpW(CO)_2LX \xrightarrow{h\nu} CpW(CO)LX + CO \qquad (2\text{-}12)$$

L=CO, PPh_3, $P(nBu)_3$, $P(OMe)_3$
X=Cl, I

The back reaction with CO in all cases is very fast, occurring at temperatures as low as at 50K. The temperature at which this reaction occurs is probably an indication of the ability of the solvent, in our case 1,2-epoxyethylbenzene, to separate the photogenerated free CO from the intermediate to prevent the possible recombination. Although, the reaction with CO occurs at low temperature, the system may be warmed up to 100K where the back reaction is still not complete.

In principle, photolysis of $CpW(CO)_3X$ should yield two intermediates, referred to as cis and trans isomers. There are two stereochemical environments for the carbonyl ligands in the complex $CpW(CO)_3X$, two of the carbonyl groups are cis to the halogen ligand and one is trans to the halogen. As shown in fig.1-5, loss of cis and trans carbonyl ligands afford two stereochemically different coordinatively unsaturated $CpW(CO)_2X$ intermediates. We call these intermediates T shaped in geometry (I and II). Interconversion of the two intermediates via III, the so called Y shaped intermediate may be possible, depending on the energy barriers for the rearrangement.

Attack at intermediate III by entering ligands should yield an approximately 67% cis-and 33% trans-$CpW(CO)_2LX$ isomeric mixture since attack between carbon monoxide and the halogen is twice as possible as attack between the two carbonyl ligands[38].

Early reports show that monosubstituted complexes having cis geometry are formed exclusively as the primary products of the photoreactions of $CpM(CO)_3X$ with PPh_3. This indicates that selective formation of cis-$CpW(CO)_2PPh_3X$ is the result of stereospecific loss of carbon monoxide cis to the halogen from $CpW(CO)_3PPh_3$. This would require that the $CpW(CO)_2X$ intermediate be stereochemically rigid during their solution lifetime before capture by PPh_3. Our results at 77K confirm this assumption. The production of only cis-$CpW(CO)_2X$ at 77K clearly shows that this T shaped intermediate is stereochemically rigid. Infrared[47] and ^{13}C NMR[48] spectral data for ground-state $CpW(CO)_3X$ complexes indicate that the bond between the metal and the cis carbonyl ligand is weaker than the bond between the metal and the trans carbonyl ligand. If these relative metal-carbonyl bond strengths persist in the excited-state complexes, then preferential loss of carbonyl ligands cis to the halogen is expected. However, it is possible that following loss of a trans carbonyl ligand from $CpW(CO)_3X$, intermediate II undergoes facile rearrangement via III to I .

The T shaped geometry of the intermediate $CpW(CO)_2X$ is confirmed by the calculated angles between the two remaining two CO ligands using equation $\tan^2\theta = Is/Ia$. These are found for the $CpW(CO)_2Cl$ and $CpW(CO)_2I$ to be 74.8° and 75.8°. In each case, these are consistent

with a T shaped geometry in which the two CO ligands adopt a cis configuration. In a Y shaped geometry , the angle should be slightly bigger as found in $CpRu(CO)_2Cl$, 92°, and in $CpFe(CO)_2I$, 91°[49].

The T shaped geometry is further indicated by the observation that the cis and trans $CpW(CO)_2LX$ molecules give rise to discreet CO loss products at 12K. Both of these intermediates are consistent with a formulation as CpW(CO)LX. They differ not only in their spectroscopic properties but also in their subsequent reactivity: each isomer of the unsaturated reacts with CO to regenerate their starting complex with specific geometry (eq.2-13 and 2-14). This again is an indication of the T shaped geometry.

$$cis\text{-}CpW(CO)_2LX \underset{\Delta}{\overset{h\nu}{\rightleftharpoons}} cis\text{-}CpW(CO)LX + CO \qquad (2\text{-}13)$$

$$trans\text{-}CpW(CO)_2LX \underset{\Delta}{\overset{h\nu}{\rightleftharpoons}} trans\text{-}CpW(CO)LX + CO \qquad (2\text{-}14)$$

The results are all consistent with CO loss to generate a rigid unsaturated fragment with a stable geometry. It appears likely that the CO is lost from one position in each case and the thermal back reaction returns the CO to that position.

Although photolysis of $CpW(CO)_3X$ results in a rigid intermediate at 77K, the electronic properties and steric requirements of phosphines are different from those of carbon monoxide. The original

location of the carbonyl ligands that dissociate is not necessarily reflected by the stereochemisty of the substituted compounds. This explains the different results for $CpW(CO)_2LX$ at 12K and at 77K.

At relatively high temperature, 77K, the isomerization barrier can be overcome. So, the change of structure from I to II is possible. Structure III , the Y shaped fragment, is the transition state for this isomerization process. The result of photolyzing $CpW(CO)_2LX$ at 77K shows the production of a mixture of I and II. This mixture then in turn produced a mixture of isomers during the CO back reaction.

The slightly different electronic properties of phosphites, compared with phosphines, give rise to another interesting result. At 77k, besides CO loss and the production of an intermediate, photolyzing of the trans-$CpW(CO)_2P(OMe)_3I$ also shows direct isomerization to the cis isomer (possibly via CO loss and follow up rearrangement). At room temperature, however, the cis isomer is not stable and easily isomerizes to the trans isomer due to the thermal stability of the trans isomer.

2.5 Summary

The photochemistry of molecules of the type $CpM(CO)_2LX$ (M = V, L = X = CO, PR_3; M = W, L = CO, PR_3, X = I) have been studied by FTIR spectroscopy at temperatures as low as 12K. For each case, CO is lost and an unsaturated intermediate is produced upon photolysis. Photolysis of $CpV(CO)_3PR_3$ resulted in a 16 electron dicarbonyl complex

$CpV(CO)_2PR_3$ with the remaining two CO's trans to each other. Further photolysis yielded a 14 electron species (Fig. 2-17). Photolysis of both cis and trans $CpV(CO)_2(PR_3)_2$ resulted in rigid intermediates which are insensitive to temperature from 12K to 77K (Fig. 2-18). Photolysis of the dicarbonyl tungsten complexes, however, resulted in temperature dependent results. At 12K, rigid intermediates were produced from both the cis and trans compounds (Fig. 2-19). At relatively high temperature, 77K, the isomerization barrier is overcome resulting in the production of a mixture of intermediates which in turn produced both isomers upon thermal back reaction (Fig. 2-20).

Up to now, we have studied the photolysis of four four-legged piano stool systems which are the rhenium system, molybdenum system, vanadium and tungsten system. They follow the same reaction mechanism, that is they all lose CO upon photolysis. However, they have differences. Both the vanadium and molybdenum compounds produce rigid intermediates, rhenium compounds yield a single intermediate for both the cis and trans starting compounds, and the tungsten compounds give temperature dependent intermediates. So isomerization is easy for third row transition metal complexes, while for first and second row transition metal molecules, more energy is required for isomerization.

In conclusion, we have shown that most three-legged photochemical intermediates are geometrically rigid at certain temperature (up to 100K in many cases). We may use these molecules for the catalytic cycle producing chiral molecules, since molecules of the type cis or trans CpM(CO)LL' (L and L' are both two electron donor ligands) are chiral intermediates and in many cases would retain their chirality.

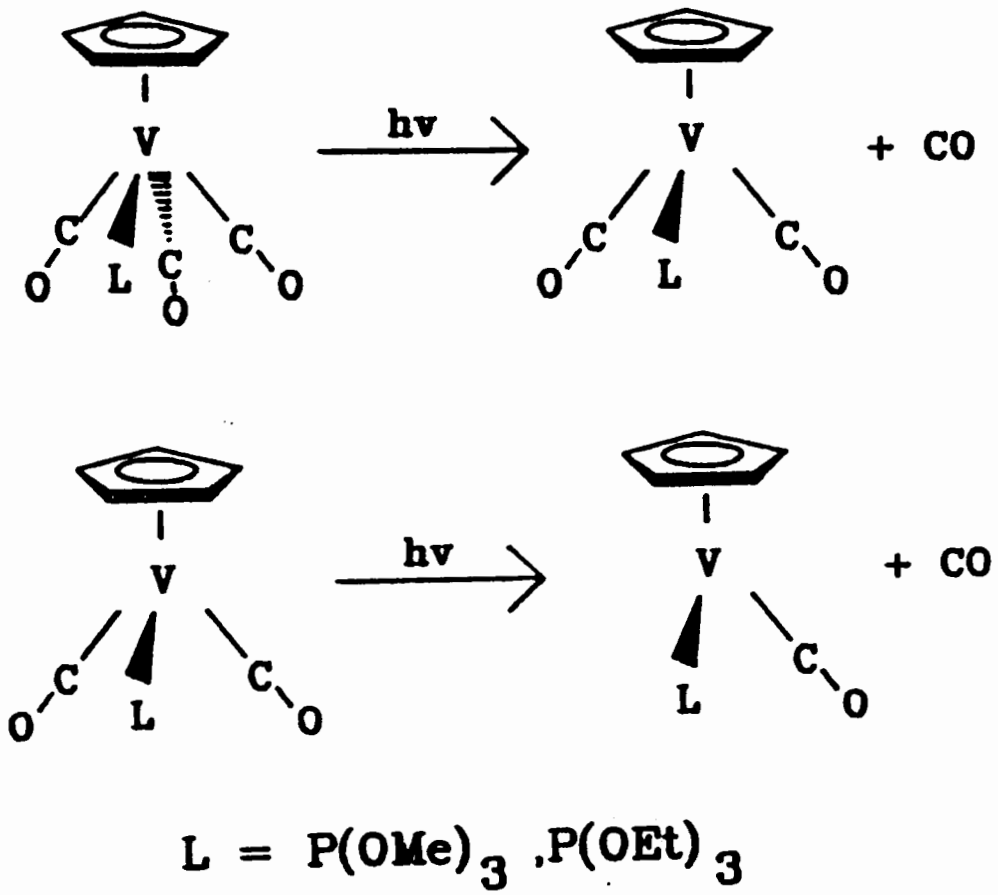

Fig. 2-17 The reaction mechanism of $CpV(CO)_3PR_3$ upon photolysis.

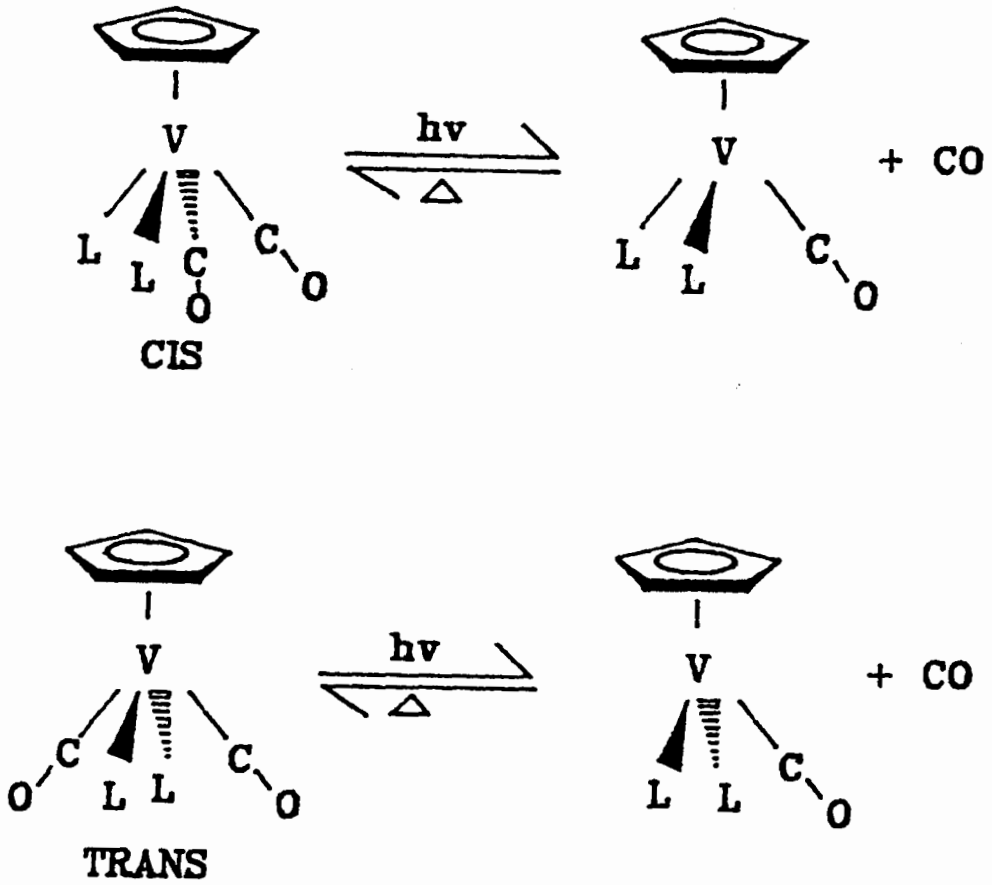

Fig. 2-18 The reaction mechanism of cis and trans $CpV(CO)_2L_2$

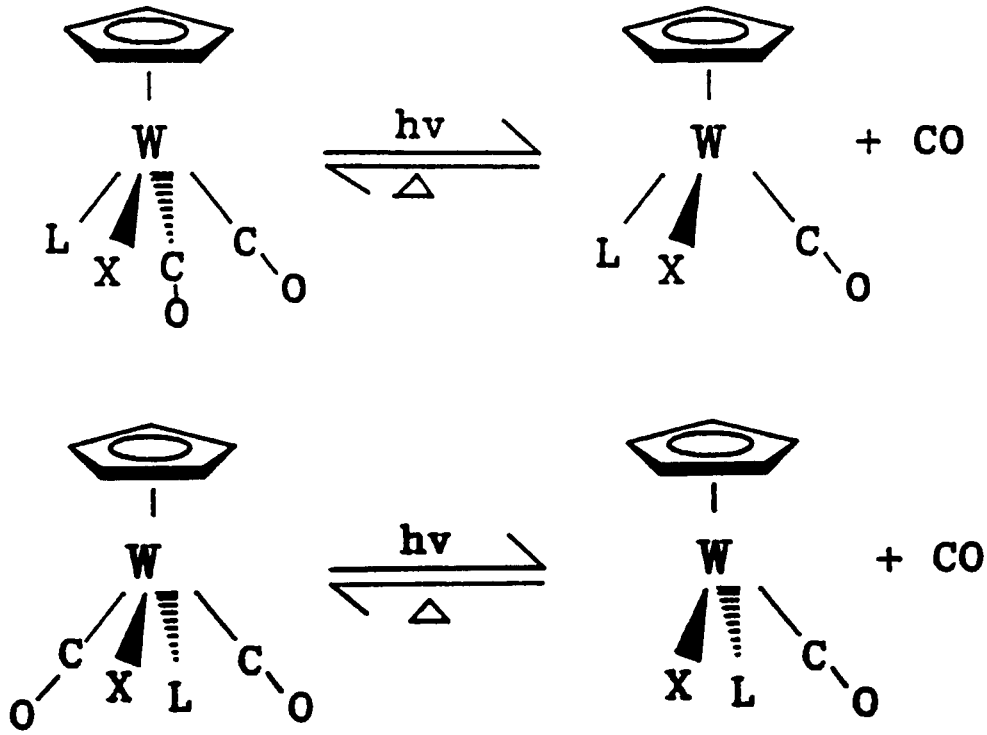

$X = I$

$L = PPh_3,\ P(nBu)_3,\ P(OMe)_3$

Fig. 2-19 the reaction mechanism of cis and trans $CpW(CO)_2LX$ at 12K

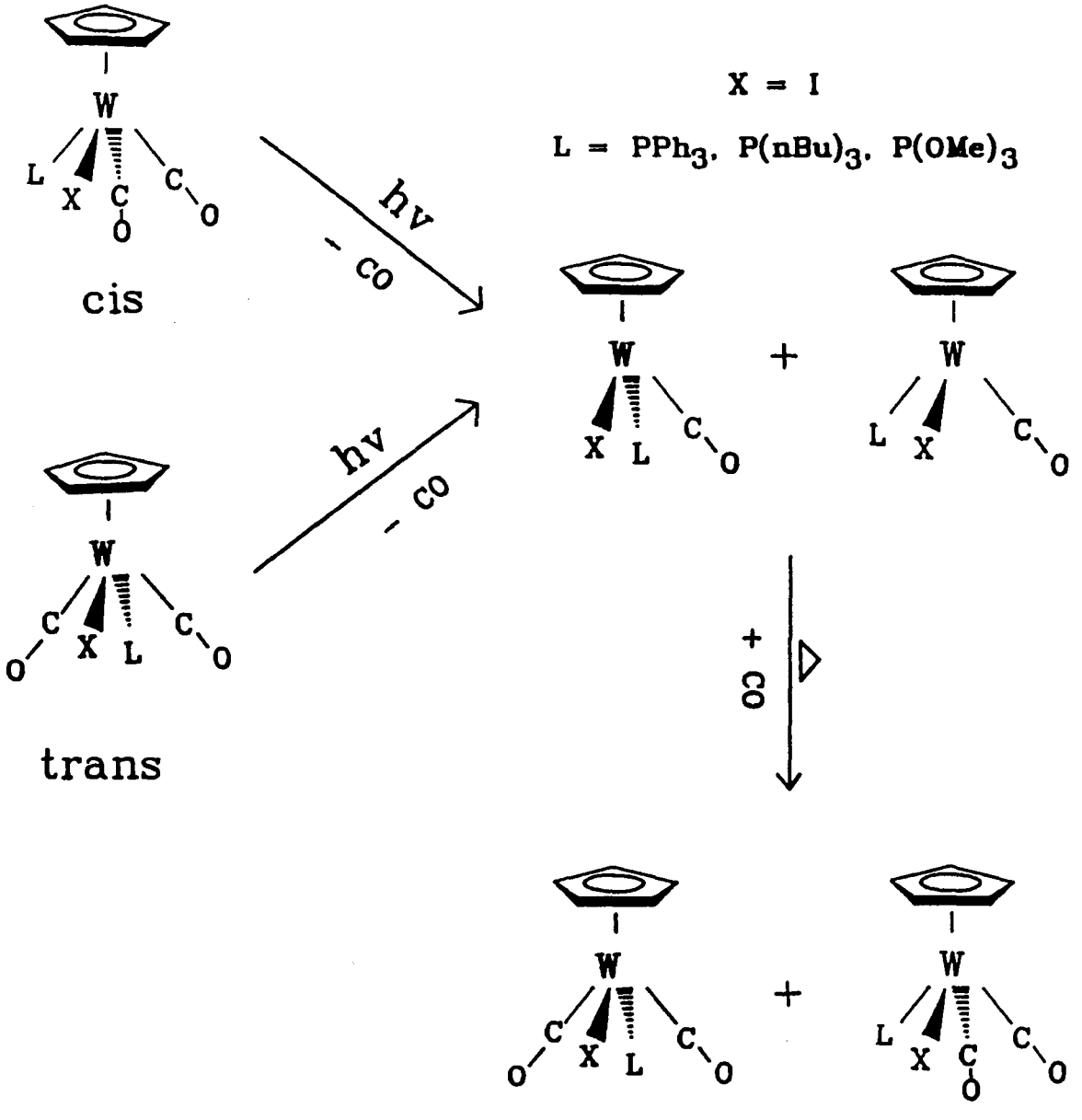

Fig. 2-20 The reaction mechanism of cis and trans-$CpW(CO)_2LX$ at 77K

Chapter3: The application of Timney's method to geometrical studies of photochemical intermediates

3.1 Some basic theory about force constants and Timney's method:

The qualitative theory concerning metal to carbon monoxide bonding in metal carbonyls involves a synergic type of bonding, that is, the bonding in these complexes can be discussed in terms of two components, C——>M dative sigma bonding and M——>C dative pi bonding[50]. The σ bond is formed by overlap of the highest filled orbital of CO (5σ) with the empty orbitals of the metal, while the π bond is formed by overlap of formally full metal d-orbitals of the correct symmetry with the lowest empty orbital of CO (2π). Both the 5σ and 2π orbitals are localized mainly on the carbon atom[52] so that one may speak of metal-carbon multiple bonding.

The vibrational spectra of metal carbonyls have proved particularly informative. The CO stretching bands observed in the infrared region are, to a good approximation, specific group frequencies. They are also sharp, sensitive to environment, and, commonly, intense. The number and pattern of the bands give information about molecular symmetry and geometry, while the positions of the bands are related to bonding[52].

In the early 60's, on the basis of symmetry-produced "factoring out" of the pi bonding and further, by more detailed consideration of the directional properties of the metal d orbitals, Cotton and Kraihanzel[53] proposed a simple model to analyze and assign

the infrared-active carbonyl stretching frequencies of simple and substituted metal carbonyls. They interpreted the theory in a semiquantitative way in regard to the CO stretching force constants, stretch-stretch force constants and, ultimately, in terms of the relative frequencies of those normal vibrations of molecules which may be regarded as pure CO stretching modes.

Following this, there were a number of proposed models and simple empirical equations based on "Energy factored Force field" proposed by Cotton and Kraihanzel.

The vibrational frequencies of a molecule are found by solving the following matrix equation (eq.3-1):

$$| FG - \lambda E | = 0 \qquad (3\text{-}1)$$

where λ is related to the molecular vibrational frequencies by the following equation (eq.3-2):

$$\lambda = 4\pi^2 c^2 \nu^2 \qquad (3\text{-}2)$$

Here, ν is the molecular vibrational frequency; F is a matrix containing the force constants of the bonds (stretching, bending) and thus describing the potential energy of the molecule; G is a matrix which is related to the kinetic energy of the molecule; and E is a unit matrix.

The CO stretching frequencies of metal carbonyls are very intense and are found in the region of the IR spectrum near $2000cm^{-1}$.

Since they are well removed from other vibrations, a high-frequency approximation is used which assumes that the νCO bands are totally decoupled from any other modes. This is called energy factoring, and the force constants derived from it comprise the "Energy Factored Force Field" or "EFFF". The method[54] involves the construction of an F matrix in the normal way from the internal coordinates, simply the changes in length for each CO group in the molecule, r_{CO}. The diagonal elements of the F matrix consist of force constants for each unique CO bond and the off-diagonal elements consist of the interaction force constants. The G matrix is one whose only non-zero elements are the diagonal ones containing the reciprocal reduced masses of CO.

The theory and application of EFFF to metal complexes has been fully evaluated by Braterman[55] and Burdett[56]. The theory has had particular success in confirming the proposed structures of matrix-isolated metal-carbonyl fragments[57]. This is a particularly useful method in those circumstances where more conventional structural methods such as X-ray crystallography are inappropriate. This is most obviously true for reactive molecules trapped in low-temperature matrices.

In the late 70's, based on the observation of Haas and Sheline[58] that ligand effects on C-O stretching force constants are additive, Timney[32] proposed a marvelously simple empirical relationship for the prediction of CO stretching frequencies in a wide variety of metal carbonyl complexes. Like others, Timney also assumed an energy-factored force field, and postulated that the C-O stretching force constant is given by the general equation (eq.3-3):

$$K_{co} = K_d + \sum_L \varepsilon_L^{\theta} \qquad (3\text{-}3)$$

Here, K_d is the force constant for an isolated monocarbonyl fragment, M-CO, and depends only on the transition series and on the formal number of d electrons on the metal. All the values were derived from either the observed frequencies of matrix-isolated metal monocarbonyl fragments[59] or empirically from the above equation. The terms ε_L^{θ}, which Timney refers to as ligand effect constants, quantify the effect on K_d of adding a particular ligand L to M-CO at angle θ.

The ligand additivity relationship proposed by Timney works remarkably well for both electronically saturated (18 electron) and unsaturated (< 18 electron) metal carbonyl complexes. For example, Timney has applied the model to the isomers of $Mo(CO)_{6-n}(PF_3)_n$ (n=0, ..., 5) and it worked quite well[60].

3.2 The application of the above theory to compounds of Chapter 2

We will apply all the above methods to our system to investigate the following:

a. From our IR results, we have predicted some of our intermediates be T shaped or Y shaped with ligand cis or trans to each other. So, by calculating the force constants for individual CO ligand and interaction force constants, we should be able to calculate the ligand effect constants. By applying these results to certain system with the geometry we assigned according to their IR behavior, particularly for the photochemical intermediates, we should be able to

confirm the assigned geometries.

b. Previously, Timney had shown that the empirical equation worked for metal carbonyls with octahedral, tetrahedral and trigonal bipyramidal geometries. We will apply the results to our piano-stool shaped molecules of either 18 electron or non-18 electron systems, to see if the empirical equation also works for systems other than θ = 90° (octahedral, ε_L^{cis}), 180° (octahedral, ε_L^{trans}), 109.5° (tetrahedral, ε_L^{td}), 90° (trigonal bipyramidal, $\varepsilon_L^{ax,eq}$), and 120° (trigonal bipyramidal, $\varepsilon_L^{eq,eq}$).

c. In the Tungsten system, the cis isomer has two possibile structures for the photochemical intermediate. One with the remaining CO trans to the phosphine and the other one with the CO ligand trans to the halogen ligand. So by doing calculations, we should be able to distinguish these two possibilities.

3.3 Data and discussion:

a. CO stretching force constants:

The force constants for an individual CO ligand and CO stretch-stretch interaction force constants for both the Vanadium and Tungsten systems have been calculated using the "carbonyl" set of programs [61]. These programs calculate the force constants and adjusts them to fit the observed frequencies by a least square method. In our case, all the IR frequencies are observed at 12K in a 1,2-epoxyethylbenzene matrix. The results are summarized in Table 3-1 and Table 3-2.

Our results are consistent with the five assumptions which

Table 3-1: FORCE CONSTANTS FOR VANADIUM COMPLEXES (Nm^{-1}):

Compound	K_1	K_2	K_{cis}	K_{trans}
$CpV(CO)_4$	1544.7	-	19.4	42.9
$CpV(CO)_3$	1472.5	1455	50.6	60
$CpV(CO)_3PPh_3$	1466.3	1392	39.4	50.2
trans-$CpV(CO)_2PPh_3$	1408.6	-	-	79.3
$CpV(CO)_3P(nBu)_3$	1432.2	1375	40.6	60
trans-$CpV(CO)_2P(nBu)_3$	1395	-	-	78
$CpV(CO)_3P(OMe)_3$	1454.6	1425.1	48.4	49.6
trans-$CpV(CO)_2P(OMe)_3$	1419	-	-	79.5
$CpV(CO)P(OMe)_3$	1518.7	-	-	-
cis-$CpV(CO)_2[P(OMe)_3]_2$	1355.6	-	55.5	-
cis-$CpV(CO)[P(OMe)_3]_2$	1330.7	-	-	-
trans-$CpV(CO)_2[P(OMe)_3]_2$	1364.1	-	-	68.4
$CpV(CO)_3P(OEt)_3$	1453.3	1422	49.7	50
trans-$CpV(CO)_2P(OEt)_3$	1414.5	-	-	79.4
$CpV(CO)P(OEt)_3$	1514.1	-	-	-
cis-$CpV(CO)_2[P(OEt)_3]_2$*	1344.5	-	57.5	-
cis-$CpV(CO)[P(OEt)_3]_2$*	1319	-	-	-
trans-$CpV(CO)_2[P(OEt)_3]_2$	1363.3	-	-	69

*: Data taken from compounds trapped in a matrix at 77K.

Table 3-2: FORCE CONSTANTS FOR TUNGSTEN COMPLEXES (Nm^{-1}):

Compound	K_1	K_2	K_{cis}	K_{trans}
cis-$CpW(CO)_2PPh_3I$	1459.6	1449.4	65.6	-
cis-$CpW(CO)PPh_3I$	1300.05	-	-	-
trans-$CpW(CO)_2PPh_3I$	1466.9	-	-	67.6
trans-$CpW(CO)PPh_3I$	1320.6	-	-	-
cis-$CpW(CO)_2P(nBu)_3I$	1444.5	1434	70	-
cis-$CpW(CO)P(nBu)_3I$	1282.95	-	-	-
trans-$CpW(CO)_2P(nBu)_3I$	1446.9	-	-	67.6
trans-$CpW(CO)P(nBu)_3I$	1293	-	-	-
cis-$CpW(CO)_2P(OMe)_3I$	1482	1465.5	62	-
cis-$CpW(CO)(POMe)_3I$	1341	-	-	-
trans-$CpW(CO)_2P(OMe)_3I$	1486.9	-	-	63.6
trans-$CpW(CO)P(OMe)_3I$	1347	-	-	-

Cotton and Kraihanzel proposed in the early 60's. In some cases, particularly for the tricarbonyl complexes, we have run into the situation where we have to adjust four force constants to fit three observed frequencies which gives the inexact solutions. In these cases, only the averaged force constants for the three carbonyls are constant and we thus used the averaged values to conduct the rest of the calculations.

Ligands with different σ donor ability and π acceptor ability have a large influence on CO stretching force constants. Previously, people have measured the electron-withdrawing ability of the L_nM metal-ligand by CO stretch force constants and predicted the susceptibility of CO ligands to nucleophilic attack[62] and reactivity of π-ethylene and π-benzene ligands with nucleophiles[63]. Our results show that the CO stretching force constants decreased steadily as CO groups are successively replaced by other ligands which make less demand for metal $d\pi$ electrons. When one CO group in $CpV(CO)_4$ was replaced by different ligands, $P(OMe)_3$, $P(OEt)_3$. PPh_3, and $P(nBu)_3$, the averaged CO force constants decreased in the order $CpV(CO)_4$ > $CpV(CO)_3P(OMe)_3$ > $CpV(CO)_3P(OEt)_3$ > $CpV(CO)_3PPh_3$ > $CpV(CO)_3P(nBu)_3$. This is consistent with the decreasing π acceptor ability of the ligands CO > $P(OMe)_3$ > $P(OEt)_3$ > PPh_3 > $P(nBu)_3$ and with the σ donor ability in the opposite order. A similar trend has been found in the series $CpV(CO)_3$, trans-$CpV(CO)_2P(OMe)_3$, trans-$CpV(CO)_2P(OEt)_3$, trans-$CpV(CO)_2PPh_3$, and trans-$CpV(CO)_2P(nBu)_3$. The trend that force constants decrease for successive CO replacement with ligands of low π acceptor ability is indeed the case. This is because when CO is

replaced by L, with lower π acceptor ability, there are more metal d electrons available to the remaining CO, hence, the back bonding to the π^* orbitals of these CO groups is stronger compared with those ones with no L ligands at all. The CO bond is then weakened and the force constant associated with it is reduced.

b. Ligand effect constants:

In order to determine the geometry of a molecule qualitatively, the ligand effect force constants are desirable. We refined all the vibrational force constants for both the Vanadium and Tungsten compounds in a least squares procedure with observed frequencies for a particular geometry using Timney's method. Table 3-3 shows the comparison of the observed force constants and the calculated ones after all the data was fit via a least squares procedure with an overall error of 2.6 Nm^{-1} (in terms of frequency, it is approximately 2.03 cm^{-1}). Table 3-4 shows the calculated ligand effect force constants for ligands cis or trans to the CO ligand in a piano-stool system.

Although there is no attempt by Timney to attach a chemical meaning to his ε_L^{θ} term, some suggested the correlation between the term and the σ and π ability of the ligands[64] since the ε_L^{θ} parameters convey the change in the CO stretching force constant of an M-CO fragment. A positive value indicates a ligand which, relative to its absence, has decreased the back bonding of the CO. Similarly, a negative value indicates a ligand whose presence is enhancing the weakening of the CO bond. In our case, we have ligands CO and I with

Table 3-3: COMPARISON OF OBSERVED AND CALCULATED FORCE CONSTANTS:

Compounds	Obsd(Nm^{-1})	Calcd(Nm^{-1})	diff(Nm^{-1})
$CpV(CO)_3PPh_3$*	1428	1428	0
$CpV(CO)_3P(nBu)_3$*	1413	1412	1
$CpV(CO)_3P(OMe)_3$*	1445	1446	-1
cis-$CpV(CO)_2[P(OMe)_3]_2$	1356	1356	0
cis-$CpV(CO)[P(OMe)_3]_2$	1331	1330	1
trans-$CpV(CO)_2[P(OMe)_3]_2$	1364	1364	0
$CpV(CO)_3P(OEt)_3$*	1443	1443	0
cis-$CpV(CO)_2[P(OEt)_3]_2$	1345	1345	0
cis-$CpV(CO)[P(OEt)_3]_2$	1319	1320	-1
trans-$CpV(CO)_2[P(OEt)_3]_2$	1363	1363	0
cis-$CpW(CO)_2PPh_3I$**	1454	1454	0
trans-$CpW(CO)_2PPh_3I$	1467	1467	0
trans-$CpW(CO)PPh_3I$	1321	1321	0
cis-$CpW(CO)_2P(nBu)_3I$ **	1439	1441	-2
trans-$CpW(CO)_2P(nBu)_3I$	1447	1445	2
trans-$CpW(CO)P(nBu)_3I$	1293	1299	-6
cis-$CpW(CO)_2P(OMe)_3I$**	1474	1472	2
trans-$CpW(CO)_2P(OMe)_3I$	1487	1488	-1
trans-$CpW(CO)P(OMe)_3I$	1347	1342	5

* Data taken as the average value of the three CO force constants.
** Data taken as the average value of the two CO force constants.

Table 3-4: OPTIMIZED LIGAND EFFECT CONSTANTS (Nm^{-1}) FOR VANADIUM AND TUNGSTEN SYSTEMS:

Ligand	ε_L^{cis}	ε_L^{trans}
CO	25	147
PPh_3	-81	41
$P(nBu)_3$	-103	36
$P(OMe)_3$	-60	54
$P(OEt)_3$	-60	43
I	65	160

Table3- 5: DETERMINATION OF STRUCTURES OF THE PHOTOCHEMICAL VANADIUM INTERMEDIATES BY FORCE CONSTANTS (Nm^{-1}):

Compound	Obsd	Calcd	
		cis	trans
$CpV(CO)_2PPh_3$	1408.6	1342(66.6)	1403(5.6)
$CpV(CO)_2P(nBu)_3$	1395	1328.5(66.5)	1381(14)
$CpV(CO)_2P(OMe)_3$	1419	1359(60)	1424(5)
$CpV(CO)_2P(OEt)_3$	1414.5	1353.5(61)	1424(9.5)

Numbers in brackets are the difference between the calculated and observed values.

both positive values for ε_L^{cis} and ε_L^{trans}, indicating that both CO and I decreased the back bonding of the M-CO fragment. Interestingly, phosphine ligands have positive values while trans to the CO ligand and negative values while cis to the CO ligand.

c. Structural determination of the photochemical intermediates:

Based on the optimized ligand effect force constants, we were able to predict the force constants for the possible geometries. Hence, comparing the calculated force constants with the observed ones, we may assign the geometry assuming that the one which gives the best agreement between observed and calculated frequencies (or force constants) is the correct geometry.

For the Vanadium system, we predicted the trans geometry for the complexes $CpV(CO)_3L$, $L=PPh_3$, $P(OMe)_3$, $P(OEt)_3$, $P(nBu)_3$ based on their relative IR intensities. By doing force constant calculations we confirm the prediction for trans geometry with an average error of less than 8.5 Nm^{-1} comparing with a cis geometry with an average error of more than 63.5 Nm^{-1}.

For the complexes $CpV(CO)_2L_2$, $L=P(OMe)_3$, $P(OEt)_3$, we confirmed an intermediate band near the solvent band which we were not quite sure of during the early studies. The calculated IR frequency is 1735.7 cm^{-1} while photolysis of the compound gives a band at 1730 cm^{-1}. Due to both the low photosensitivity of the compound and the possibility of overlap of the intermediate band with the solvent band, this conclusion still remains questionable. Although the latter situation can be solved by adding the solvent peak back to the

different spectra after photolysis , this is still not very clear due to the sensitivity of the starting material and the poor signal to noise ratio.

The data for the Vanadium system is summarized in Table 3-5 while Table 3-6 shows the observed and calculated force constants for determination of the photochemical Tungsten intermediates.

In the Tungsten system, due to the presence of both a halogen ligand, I, and a phosphine ligand, there are two possibilities for the structure of complexes $CpW(CO)LI$, L= PPh_3, $P(OMe)_3$, $P(nBu)_3$, one with the remaining CO trans to I, the other one with CO trans to L. Surprisingly, from our calculated force constants, it seems that neither of the structures have a value near to the observed values. So, we think of a solvated species, that is, the solvent, 1,2-epoxy-ethylbenzene, takes the so called vacant place. In this case, in the force constant expression, we should include a solvent term either cis or trans to the compound depending on the position of the ligand L in the compound. By closely looking at the data, the solvent term ε_s^{cis} at about -114 $Nm^{-1}$is found as a common value for the complexes $CpW(CO)LI$, L = PPh_3, $P(nBu)_3$, with CO trans to I and $CpW(CO)P(OMe)_3I$ with CO trans to $P(OMe)_3$. The different structural arrangement for Tungsten complexes with phosphines as opposed to phosphites is not surprising because of the slightly different electronic properties of the two ligands.

We then readjusted the force constants in a least square way for all the Vanadium and Tungsten complexes including the

Table 3-6: DETERMINATION OF STRUCTURES OF THE PHOTOCHEMICAL TUNGSTEN INTERMEDIATES BY FORCE CONSTANTS (Nm^{-1}):

Compound	Obsd	Calcd	
		I | W—PR_3 | CO	PR_3 | W—I | CO
cis-CpW(CO)PPh_3I	1300.1	1416(116)	1443(143)
cis-CpW(CO)P(nBu)$_3$I	1283	1394(111)	1438(155)
cis-CpW(CO)P(OMe)$_3$I	1341	1437(96)	1456(115)
CpW(CO)$_2$I	1486.5	1522(35.5)	1549(62)

Numbers in brackets are the difference between the calculated and observed values.

Table 3-7: LIGAND EFFECT CONSTANTS (Nm^{-1}) AFTER CORRECTION:

Ligand	ε_L^{cis}	ε_L^{trans}
CO	25	148
PPh_3	-78	40
P(nBu)$_3$	-98	30
P(OMe)$_3$	-60	57
P(OEt)$_3$	-61	47
I	64	163
S	-114	-

S stands for solvent, 1,2-epoxyethylbenzene.

Table 3-8: OBSERVED AND CALCULATED FORCE CONSTANTS (Nm^{-1}) AFTER CORRECTION:

Compounds	Obsd	Calcd	diff
$CpV(CO)_3PPh_3$ *	1428	1428	0
trans-$CpV(CO)_2PPh_3$	1300	1302	-2
$CpV(CO)_3P(nBu)_3$ *	1413	1412	1
trans-$CpV(CO)_2P(nBu)_3$	1395	1386	9
$CpV(CO)_3P(OMe)_3$ *	1445	1446	-1
trans-$CpV(CO)_2P(OMe)_3$	1419	1423	-4
cis-$CpV(CO)_2[P(OMe)_3]_2$	1356	1357	-1
cis-$CpV(CO)[P(OMe)_3]_2$	1331	1331	0
trans-$CpV(CO)_2[P(OMe)_3]_2$	1364	1363	1
trans-$CpV(CO)[P(OME)_3]_2$	1209	1212	-3
$CpV(CO)_3P(OEt)_3$ *	1443	1442	1
trans-$CpV(CO)_2P(OEt)_3$	1414	1421	-7
cis-$CpV(CO)_2[P(OEt)_3]_2$	1345	1346	-1
cis-$CpV(CO)[P(OEt)_3]_2$	1319	1321	-2
trans-$CpV(CO)_2[P(OEt)_3]_2$	1363	1361	2
trans-$CpV(CO)[P(OMe)_3]_2$	1209	1210	-1
cis-$CpW(CO)_2PPh_3I$ **	1454	1454	0
cis-$CpW(CO)PPh_3I$ ***	1300	1302	-2
trans-$CpW(CO)_2PPh_3I$	1467	1469	-2
trans-$CpW(CO)PPh_3I$	1321	1321	0
cis-$CpW(CO)_2P(nBu)_3I$ **	1439	1440	-1
cis-$CpW(CO)P(nBu)_3I$ ***	1283	1283	0
trans-$CpW(CO)_2P(nBu)_3I$	1447	1450	-3
trans-$CpW(CO)P(nBu)_3I$	1293	1301	-8
cis-$CpW(CO)_2P(OMe)_3I$ **	1474	1472	2
cis-$CpW(CO)P(OMe)_3I$ ***	1419	1423	-4
trans-$CpW(CO)_2P(OMe)_3I$	1487	1487	0
trans-$CpW(CO)P(OMe)_3I$	1347	1339	8

* data taken as the averaged force constants of the three CO ligands.
** data taken as the averaged force of the two CO ligands.
*** compounds in which the solvent effect terms are taken into account.

intermediates with correctly assigned geometries. The solvent effect term is also taken into consideration. The results are shown in Table 3-8 with an overall error of 3.7 Nm^{-1} (or 2.91 cm^{-1} in terms frequency) and Table 3-7 are the readjusted ligand effect constants after including all the compounds. These values then give better agreement between calculated and observed frequencies than observed previously.

One more thing we should mention here is the solvent effect constant trans to CO is also calculated which is considered very small, i.e. only 5 Nm^{-1}, and the overall standard deviation remains as 3.7 Nm^{-1} after including the ε_s^{trans} term. Therefore, the solvent effect constant ε_s^{trans} is not as significant as ε_s^{cis}, but since those intermediates with CO cis to the solvent are considered as solvated, it is also not unreasonable at all that the intermediates with CO trans to the solvent are solvated with only a small solvent effect constant.

3.4 Summary

Force constants and ligand effect constants have provided a simple method to correctly assign the geometry for photochemical intermediates trapped in low temperature matrices. We have correctly assigned the geometries of $CpV(CO)_2L$, L= PPh_3, $P(OMe)_3$, $P(OEt)_3$, and $P(nBu)_3$ as trans for the remaining two CO's based on both their IR intensities and force constants calculated. In the tungsten system, a solvated situation is possible with a solvent effect constant cis to CO as -114 Nm^{-1} and trans to CO as 5 Nm^{-1}. A different geometry is observed for the tungsten intermediate of the type cis-CpW(CO)LI, for

L = phosphines versus phosphites.

From these force constant calculations, we also conclude that the interaction between the intermediate and the solvent is strong in some cases, i.e., when the solvent is cis to the CO ligand in the intermediate, and weak in other cases, i.e., when the solvent is trans to the CO in the intermediate.

Chapter 4: Semiquantitative study of the geometries of photochemical intermediates by EHMO

4.1 Introduction:

The Huckel molecular orbital (or HMO) method is a simple but powerful approach toward explaining the stabilities, physical properties, and chemical reactivities of organic π-systems. The σ-electronic framework of these systems are relatively uninteresting in a theoretical sense since the properties of σ bonds do not vary significantly from structure to structure[65]. The HMO results that one can obtain easily, are crude and approximate, being based on a number of gross assumptions or approximations. However, these results are capable of explaining and predicting a large number of interesting chemical results in a semi-quantitative way.

Although the HMO method has long been employed in the organic area, especially for those with large π systems, there are a few examples in the organometallic field[66, 67].

Based on the simple Huckel approach, Hoffmann[30] in the early 60's extended it to EHMO method, that is the so-called extended Huckel method. This method is widely employed, and in many cases a very useful extension of the simple Huckel method. It has been applied to hydrocarbon systems and is very useful for estimating energies and conformational stabilities. However, it is less useful for heteroatom systems and for estimating charge distributions. Like the simple Huckel approach, the EHMO treatment is an electron-free type of LCAO-MO

calculation, that is to say the electrons are not inserted into the MO's until the calculation of their energy levels is complete. Thus the occupancy pattern of the various MOs has no effect on their energies, so that in such methods electron-electron repulsion terms are totally neglected in any explicit way.

4.2 An outline of EHMO theory

The basic approach used in the EHMO methods is as follows[68]:

(1) All atoms in the molecular system are taken into account.

(2) the basis set is formed from Slater-type[69] atomic orbitals.

(3) All orbitals on each atom that are part of its valence shell are included in the calculations, whether these AOs are occupied in the free atom or not.

(4) The secular determinant is set up as the simple Huckel method, but all off-diagonal elements are retained (i.e., no assumptions are made about any of these being zero). Thus each matrix element is of the form $[H_{ij} - \varepsilon S_{ij}]$, whether i=j or not.

(5) Overlap integrals S_{ij} are calculated between all pairs of orbitals ϕ_i and ϕ_j on all pairs of atoms, not just nearest neighbors. Thus no intergals S_{ij} are assumed to be zero, although some may in fact turn out to be zero.

(6) It is necessary to know the molecular geometry, i.e. bond lengths and bond angles, in order to correctly calculate S_{ij} values. Thus the coordinates of all atoms must be specified.

(7) The energies of electrons in isolated AOs, which

correspond to the terms H_{ii} in the calculations, can be approximated on a scale relative to an electron at infinity by using suitable ionization potentials and electron affinities.

(8) The bond integrals are assigned numerical values based on the Wolfsberg-Helmholtz approximation[70] (eq.4-1), where

$$H_{ij} = K. \frac{[H_{ii} + H_{jj}]}{2} . S_{ij} \qquad (4\text{-}1)$$

the value of the constant K , which is used as a scaling factor, is 1.75, although the final results are not very sensitive to the precise value of K used.

On the above basis, the complete secular determinant is then solved to obtain the eigenvalues and the coefficients.

There are a number of examples of the application of EHMO calculations to organometallics. Most of these are by Hoffmann. For example, he and his coworkers have employed the EHMO method to explain and understand the barriers to internal rotation in cyclic and acyclic polyenes bonded to an ML_3 transition metal fragment[71]. This is a rare example of a study of reaction barriers on these compounds although there are many studies on bonding and reactivities of those complexes.

4.3 The application of the EHMO method

Previously, we've shown some of our 16 electron photochemical intermediates of the type $CpV(CO)L_2$, L = $P(OMe)_3$ and $P(OEt)_3$ are T shaped on the bases of their IR behavior and on the force constant calculations. However, consideration of steric factors indicates that the alternative geometry, Y shaped, should be preferred. This lies in the fact that there is a large repulsion force between the large ligands, L. Another possibility is that the solvent, 1,2-epoxyethylbenzene, could coordinate with the metal at the vacant site of the primary photoproduct. This would result in an 18 electron species with solvent in one of the coordination sites. Although conventionally, X-ray diffraction could reveal the real structure of the compounds, it is impossible to get a structure from species trapped in a low temperature matrix. In order to answer the above questions, particularly which factors (steric or electronic) are important in determining the preference of one geometry over the other, we conducted the following MO calculation based on the EHMO method by using the weighted Hij formula.

The weighted Hij formula is defined as follows[72] (eq.4-2):

$$Hij = [K - (K - 1)\Delta^2]\frac{Sij}{2}[(1 + \Delta)Hii + (1 - \Delta)Hjj] \qquad (4\text{-}2)$$

Where K is a constant as in the normal Huckle formula and Δ is defined as in equation 4-3.

$$\Delta = \frac{Hii - Hjj}{Hii + Hjj} \qquad (4\text{-}3)$$

This weighted Hij formula gives more reasonable results for organometallic systems due to the assumption that the overlap density $\phi_i\phi_j$ between orbitals i and j on different centers is a weighted average of the orbital densities $\phi_i\phi_i$ and $\phi_j\phi_j$. The normal Huckel formula assumes similar orbital "diffuseness" in molecules. The latter, however, worked fairly well in molecules where all of the basis orbitals have reasonably large occupation numbers and similar energies, e.g. organic molecules. In molecules where this condition is not met, e.g. transition metal complexes containing unoccupied, high energy s and p basis functions, the simplification of equal "diffuseness" is questionable. The obvious solution to this problem is to assume $\phi_i\phi_j$ is weighted in favour of the more contrated orbital. Our system has a transition metal, Vanadium, with unoccupied 4s and 4p orbitals, hence the use of the weighted Hij formula seems quite reasonable.

4.4 Computational methods:

Extended-Huckel molecular orbital calculations were performed by using Hoffmann's program (ICON, Version 8). The Hii's for Vanadium were obtained from a charge iteration calculation on $CpV(CO)(PH_3)_2$. The values are: 4s, -8.01 ev; 4p, -4.48 ev and 3d, -8.56 ev. The metal orbital exponents for the 3d, 4s and 4p atomic orbitals were taken

from previous work by Hoffmenn[73]. The Hii's and orbital exponents for all the atoms in the molecule are listed in Table 4-1. The weighted Hij formula with k = 1.75 was used in all the calculations. The coordinates for all the atoms were calculated by using idealized bond length and bond angles as follows in Table 4-2.

4.5 Results and Discussion:

Initial calculations were performed with a 16 electron hypothetical molecule $CpV(CO)(PH_3)_2$ with a C_{3v} bond geometry about the CpV axis (Fig.4-1). The angle between any two ligands projected onto the xy plane is 120°.

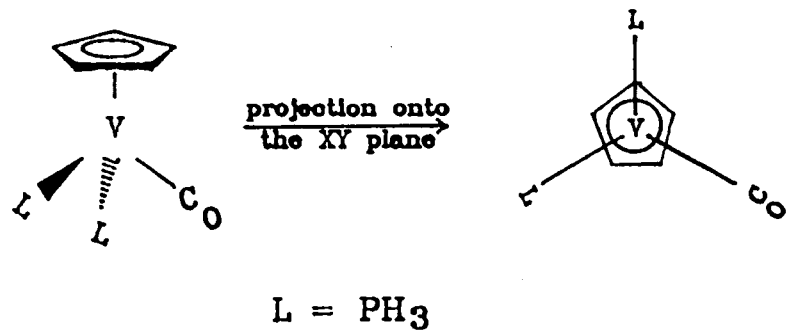

Fig.4-1 The structure of $CpV(CO)(PH_3)_2$ and its projection onto the XY plane

The EHMO calculation was performed on this molecule. An orbital interaction diagram is shown in Fig.4-2. The complex has been divided into cyclopentadienyl anion (Cp^-) and $V(CO)(PH_3)_2$ cation

Table 4-1: STANDARD Hii's AND SLATER EXPONENTS AND COEFFICIENTS:

ATOM	orbital	H_{ii}(ev)	ξ_{i1}	C1	ξ_{i2}	C2	Ref
C	2s	-21.4	1.625				78
	2p	-11.4	1.625				
H	1s	-13.6	1.3				78
O	2s	-32.3	2.275				
	2p	-14.8	2.275				78
P	3s	-18.6	1.75				79
	3p	-14.0	1.30				
V	4s	-8.01	1.30				
	4p	-4.48	1.30				
	3d	-8.56	4.75	0.4755	1.70	0.7052	41

* H_{ii}'s for V was calculated by the charge iteration method in our lab.

Table 4-2: IDEALIZED BOND LENGTH AND BOND ANGLES:

	BOND LENGTH (A°)	Ref
V-C	1.91	80
V-P	2.44	81
C-O	1.15	80
V-Cp	2.00	80
P-H	1.40	81
C-C	1.40	80
C-H	1.09	80
	BOND ANGLE (°)	
C-V-Cp	118	80
P-V-Cp	127	81
O-V-Cp	119	80
V-P-H	120	81
H-P-H	109	81
C-C-C	108	80

fragment. The orbitals at left are those of the Cp fragment which is constructed from those Pz orbitals on the five carbons of the Cp ring. The orbitals at right are those of the $V(CO)(PH_3)_2$ fragment which can be easily constructed by considering the $V(CO)(PH_3)_2$ in a C_{3v} bond geometry (the detailed derivation of the molecular orbitals for a ML_3 fragment has been given in one of previously[74]). Here we give a qualitative account of the derived MO's of the $V(CO)(PH_3)_2$ fragment.

Three low-lying orbitals, a_1 + e, are comprised mainly of z^2 ($1a_1$), xy, and $x^2 - y^2$(1e). Since the three ligands are not the same, the three orbitals are not degenerat, however, to a simple approximation, we still draw them as if they are degenerat. At somewhat higher energy, there is an e set of largely xz and yz character(2e) which are antibonding to the σ levels of the ligands. Finally, at still higher energy, there is a sp hybrid orbital. As mentioned in the previously literature[41, 75, 76], there is an intermixing between the e sets (1e and 2e)[12], or in other words, there is mixing between xy and xz and between $x^2 - y^2$ and yz in the e sets, this intermixing causes the tilting of the xy, xz, yz and $x^2 - y^2$ orbitals from their axes. Furthermore, there is some mixing of the metal p character in the 2e sets.

The a_2" orbital of Cp^- and $1a_1$ and $2a_2$ from $V(CO)(PH_3)_2^+$ enter into a three orbital pattern. The lowest molecular level is primarily a_2" stabilized by $1a_1$ and $2a_1$. The middle member is mainly $1a_1$. Some a_2" character mixes into the molecular orbital in an antibonding manner. Furthermore, $2a_1$ mixes into it in second order

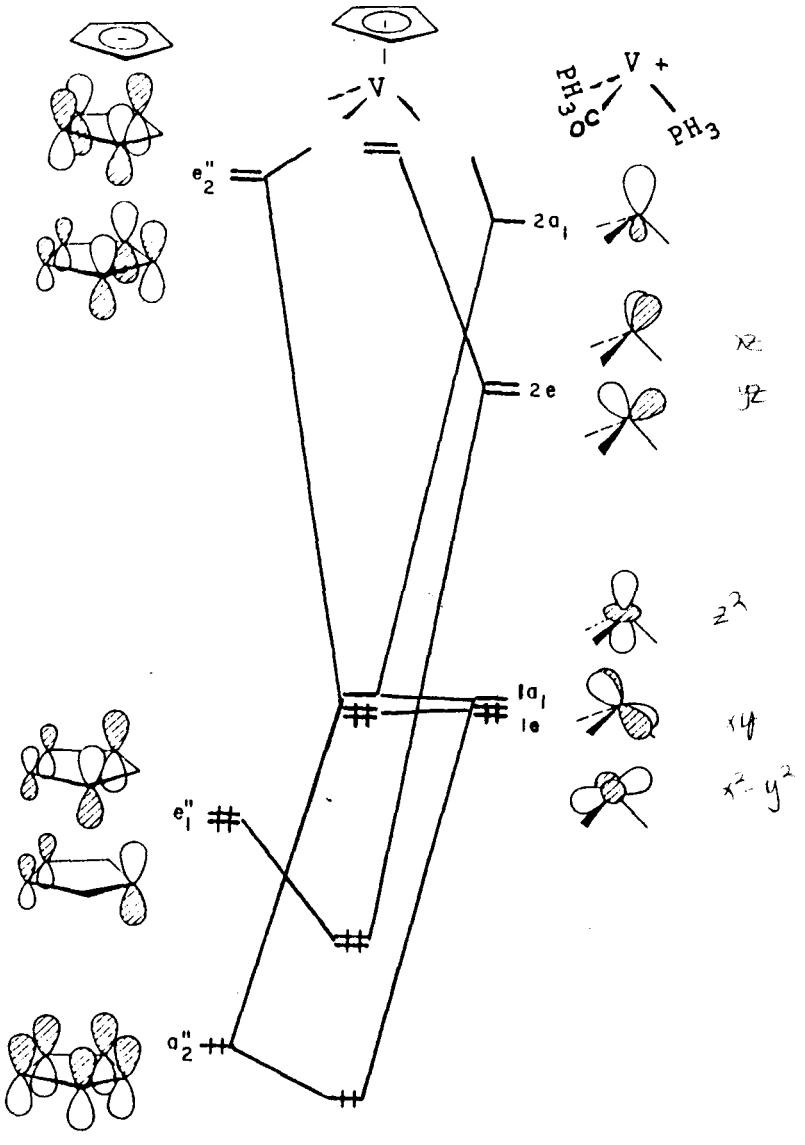

Fig.4-2 Orbital interaction diagram of Cp^- and $V(CO)(PH_3)_2^+$

(bonding with respect to a_2"). It is the second order mixing that keeps $1a_1$ at moderate energy. The e_1" set of Cp^- is stabilized greatly by 2e on $V(CO)(PH_3)_2^+$. Finally, there is a weak interaction between the 1e and e_2" levels. That stabilizes the 1e set, but not a great deal. The reason for the weak interaction between the two is explained as follows. First of all, the overlap between 1e and e_2" is primarily of the δ type and consequently is much smaller than the π type of interaction between e_1" and 2e or the σ type in the $1a_1$ + $2a_1$ + a_2" combinations. Secondly, there are relatively high lying σ orbitals on the Cp fragment which overlap with and destabilize the 1e set. Therefore, the 1e and $1a_1$ based molecular levels are not expected to be split apart significantly in energy. In our case, the HOMO and LUMO are separated by 1.21eV in energy.

By looking into the detail of the wavefunctions of the molecule, we found that our LUMO molecular orbital is dominated by the dz^2 on the metal with a small amount of mixing from dxy, dyz and some orbitals on the PH_3. There is little interaction between the metal and the CO ligand in this orbital. The HOMO orbital is dominated by the dxy on the metal with large interaction with the CO π^* orbitals and only little with the PH_3 ligands.

IR results and force constant calculations indicated the 16 electron photochemical intermediates are stereochemically rigid to 100K. If this is true, then we expect a distortion of the geometry of the intermediate from $\theta = 120^\circ$ should result in two minima on the energy surface as the result of angle variation.

In our more general study of the above system, we've explored

the most stable geometry of both the cis and trans intermediates allowing the angles (θ and α, see Fig.4-3) to vary between 80° and 180°. The variation of angle θ corresponds to the change of geometry

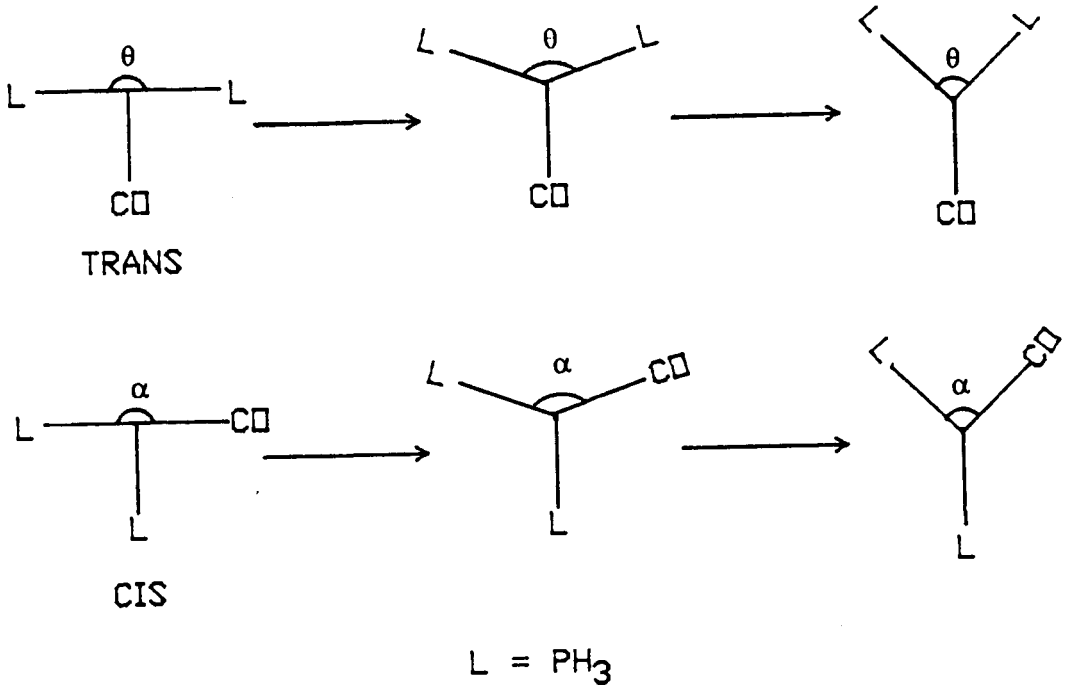

Fig. 4-3. The series of angle variation for both cis and trans isomers

for the trans complex from the ideal T (with an angle 180° for the two ligands.trans to each other) shaped geometry to a Y shaped one while the change of the angle α corresponds to the modification of the geometry for the cis isomer, again, from the T shaped to the Y shaped ones. Angles smaller than 80° are not considered here since the H atoms on PH_3 interact when the two PH_3 ligands get closer to each other resulting in a rapid raising of the total energy of the molecule.

The change of energy levels for the HOMO and LOMO orbitals with the change of the angles θ and α are summarized in Table 4-3 and 4-4. The change of the total energy for the molecule are also summarized there. Fig.4-4 and 4-5 are the Walsh[77] diagrams of the HOMO, LUMO and total energy of the above changes.

Although the HOMO and LUMO energy drops from θ = 180° to 80°, the total energy favors the geometry of the trans compound when θ reaches 130°. This is a distorted T shaped intermediate. For the cis isomer, however, we did not get the same result with α = 130°. Though the HOMO orbital favors α from 130° to 110°, the total energy reveals that the most stable geometry is the one when α reaches 110°. These results show that the intermediate of the type $CpV(CO)L_2$ does have two distinct geometries for the trans and cis isomers.

Because both the cis and trans intermediates are stable in the low temperature matrix (12K), one may expect an energy barrier for the transition from one geometry to the other. More calculations were conducted on those geometries which may lead to the isomerization from one geometry to the other. The results are summarized in Fig.4-6. All the intermediate geometries between cis and trans isomer have a higher energy and the energy barriers are: 0.01ev (-8 Kj at 12K) for the trans isomer and 0.08ev for the cis isomer. The cis intermediate is calculated to be more stable than the trans intermediate, this reveals the thermal stability of the two isomers. There is an energy barrier for the isomerization at 12K consistent with the rigidity of the intermediate from photolysis of both the cis and trans complexes.

Table 4-3: ENERGY(ev) LEVELS1 OF THE TRANS GEOMETRY AS A FUNCTION OF θ.

θ	HOMO	LUMO	SUM
180	-9.61	-8.53	-983.78
170	-9.73	-8.58	-984.55
160	-9.80	-8.61	-985.19
155	-9.82	-8.63	-985.41
140	-9.87	-8.67	-985.93
130	-9.90	-8.70	-985.99
120	-9.91	-8.71	-985.98
110	-9.94	-8.73	-985.58
100	-9.95	-8.75	-984.57
90	-9.96	-8.77	-982.68
80	-9.97	-8.80	-978.37

Table 4-4: ENERGY(ev) LEVELS1 OF THE CIS GEOMETRY AS A FUNCTION OF α.

α	HOMO	LUMO	SUM
180	-9.54	-8.58	-981.05
170	-9.69	-8.64	-982.65
160	-9.79	-8.67	-983.85
150	-9.85	-8.70	-984.66
140	-9.89	-8.71	-985.28
130	-9.93	-8.72	-985.76
120	-9.93	-8.71	-985.97
110	-9.93	-8.70	-986.06
100	-9.80	-8.69	-985.68
90	-9.66	-8.67	-985.16
80	-9.45	-8.65	-984.25

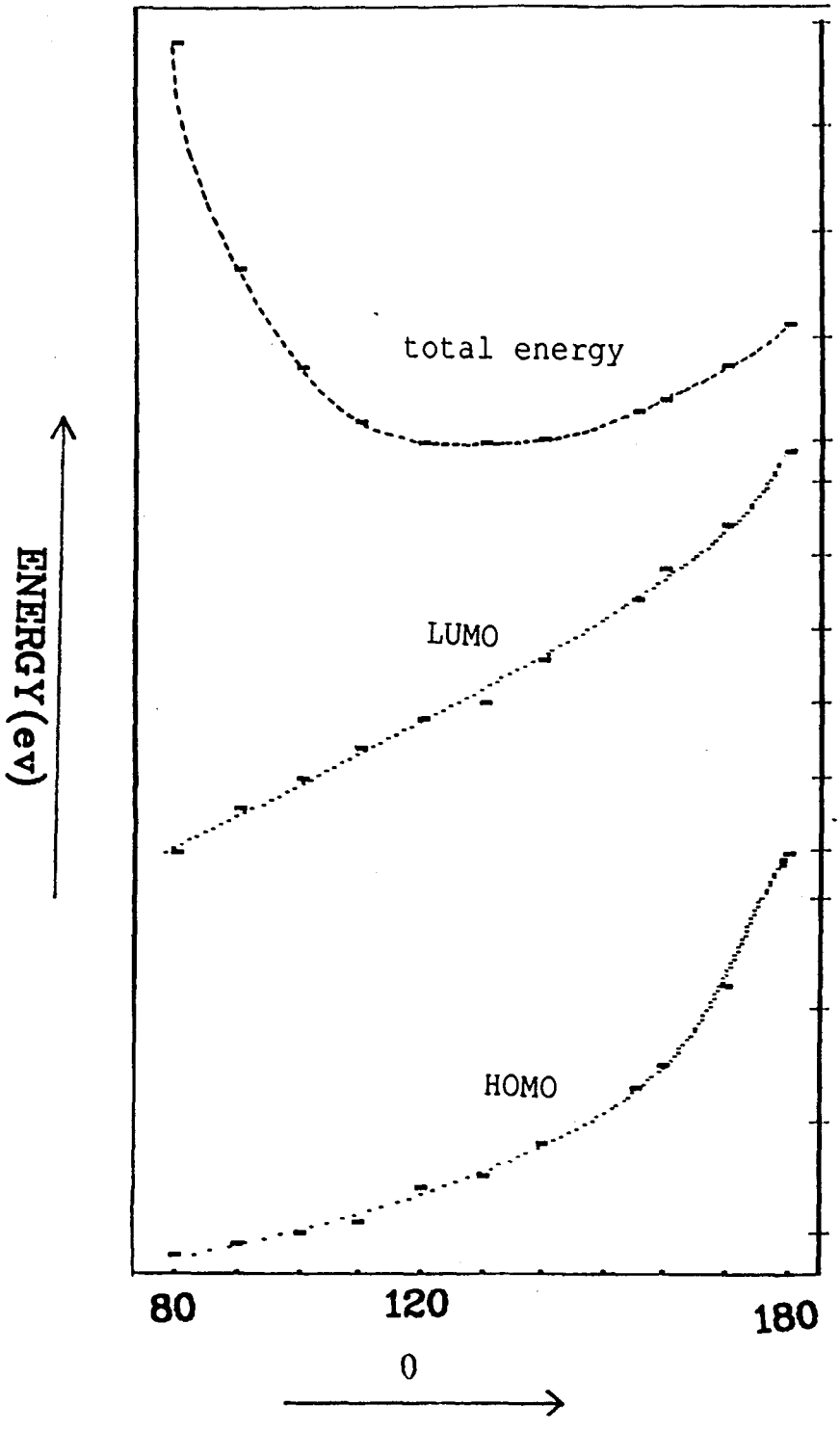

Fig.4-4 Walsh diagram of the HOMO, LUMO and total energy changes for the trans intermediate

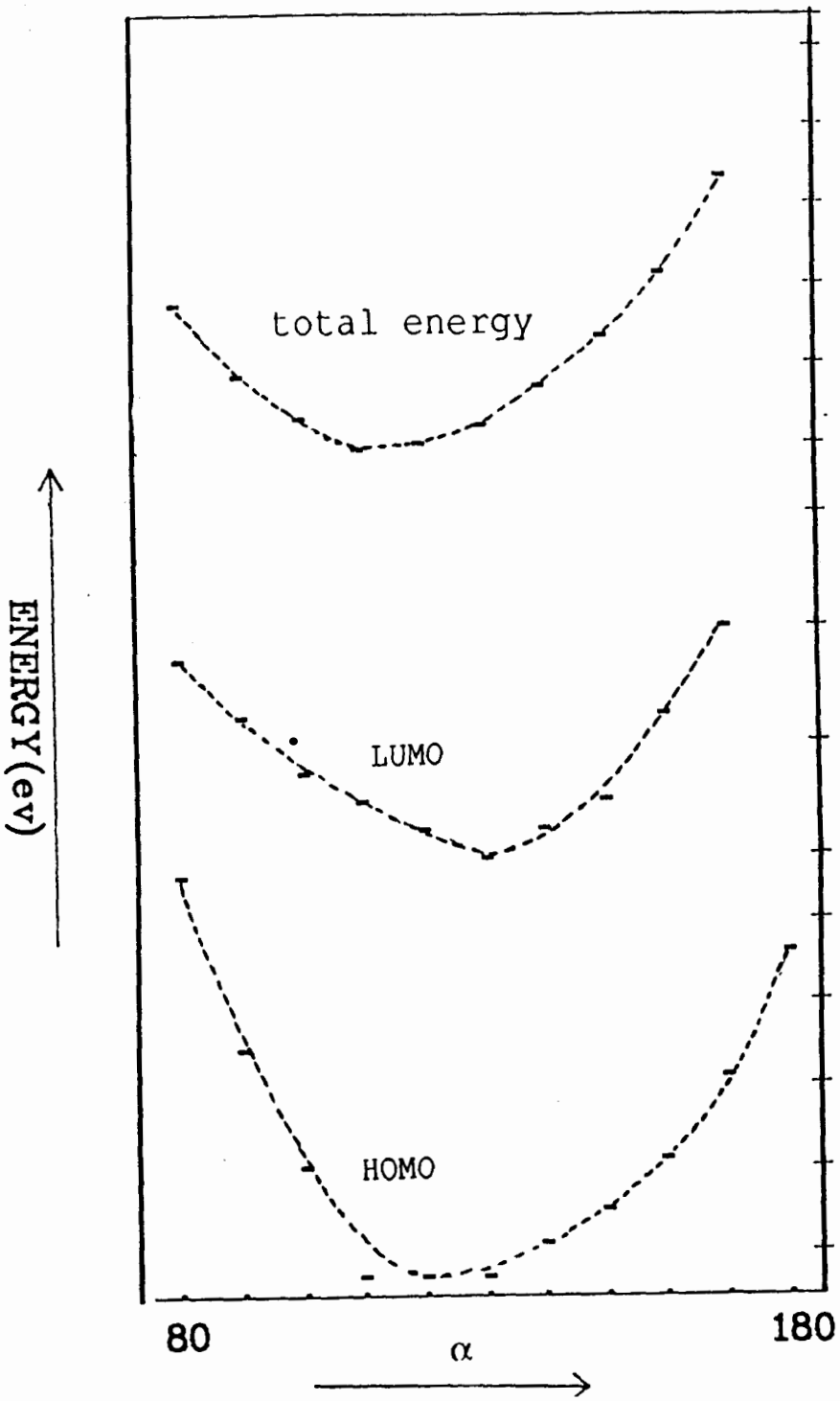

Fig.4-5 Walsh diagram of the HOMO, LUMO and total energy change for the cis intermediates

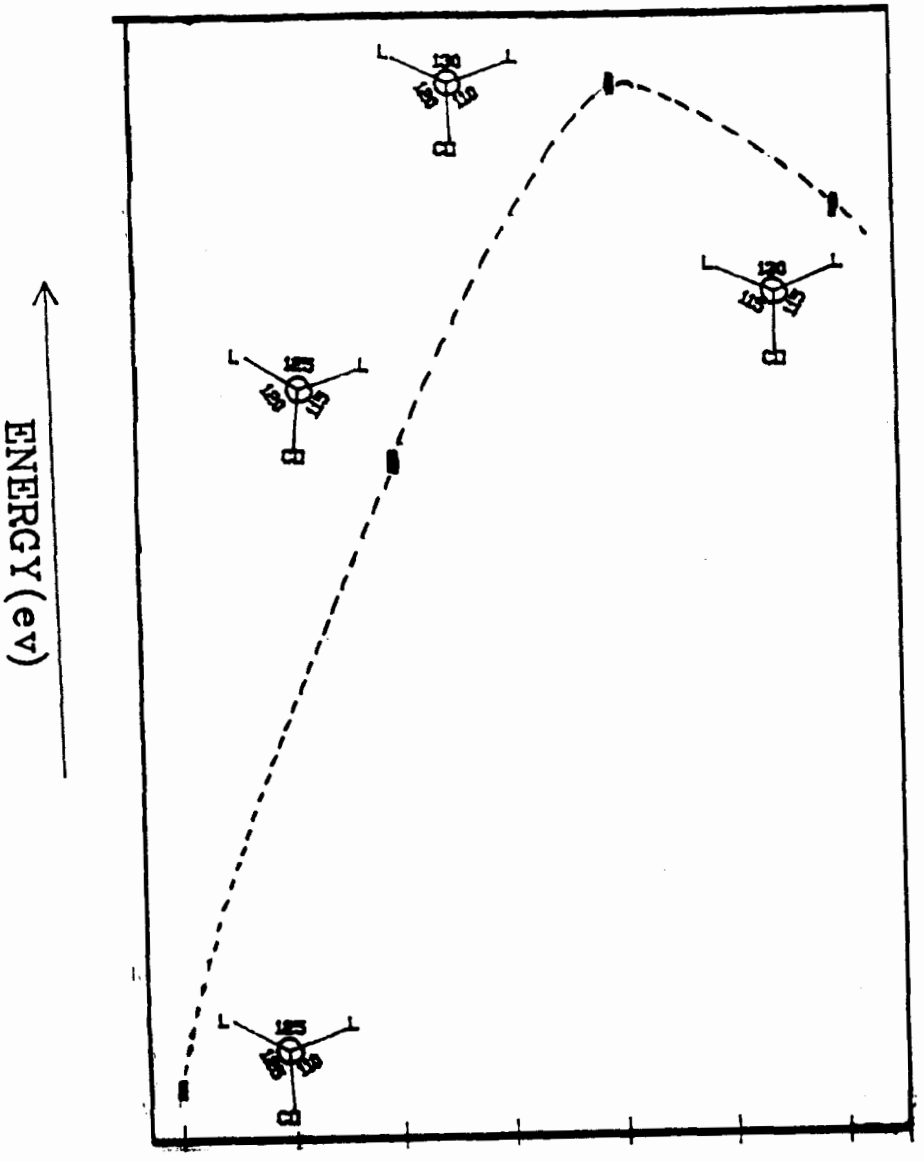

Fig.4-6 Energy barrier is expected for the isomerization process

Chapter 5: Experimental methods

5.1 Synthesis:

$CpV(CO)_4$ was purchased from Strem Chemical Co. and was used without further purification. All the vanadium complexes were prepared by irradiating $CpV(CO)_4$ with an appropriate amount of ligand in distilled tetrahydrofuran solution (eq.5-1)[34].

$$CpV(CO)_4 + nL \xrightarrow[THF,\ 60°]{h\nu} CpV(CO)_{4-n} + nCO \qquad (5\text{-}1)$$

L= $P(OMe)_3$, $P(OEt)_3$, PPh_3, $P(nBu)_3$

Here, n=1 or 2 corresponds to the monosubstituted complex or the disubstituted complex. The initial mixture products, including $CpV(CO)_3L$ and cis or trans $CoV(CO)_2L_2$ are then purified by column chromtography. This was done by passing the solutions (evaporated to about 5ml) through 1.5cm x 30cm column packed with silica gel(60-200 mesh), using benzene-hexane mixture as eluant (1:5 benzene-hexane mixture for $CpV(CO)_3L$ and approximately 1:1 mixture used for separating the cis and trans $CpV(CO)_2L_2$.

$CpW(CO)_3Cl$ was prepared by ultraviolet irradiation[35] of $[CpW(CO)_3]_2$ in CCl_4 solution under nitrogen for about 10 minutes. The product was again separated and purified from the tungsten dimer by passing the solution through a column packed with alumina using dichloromethane as the eluant. $CpW(CO)_3I$ was prepared by a similar

method, except CHI_3 was used instead of CCl_4.

All the cis and trans tungsten dicarbonyl compounds were prepared by irradiating $CpW(CO)_3X$ with the corresponding ligand and the tungsten dimer in tetrahydrofuran solution (eq.5-2)

$$CpW(CO)_3X + L \xrightarrow[THF]{[CpW(CO)_3]_2} \textit{cis or trans}\text{-}CpW(CO)_2LX + CO \qquad (5\text{-}2)$$

L = PPh_3, $P(nBu)_3$, $P(OMe)_3$
X = I, Cl

The use of tungsten dimer here involves a radical reaction process in which the trans isomer yield will be increased[38]. The cis and trans mixtures are separated and purified by column cromotography using alumina and 2:3 hexane-dichrolomethane mixture as eluant.

5.2 Spectra:

All FTIR spectra at 12K were obtained with a Bruker IFS 85 spectrophotometer. The samples were cooled in CaF_2 IR cells using a CTI cryogenics model 22 cryocooler and a 350R compressor system equipped with a Lake Shore cryotronics DRC80C temperature controller. The temperature was monitored with a Lake Shore cryotronics silicon diode sensor.

All the FTIR spectra at 77K are obtained with a Boman Michelson FTIR machine. Samples are cooled with liquid nitrogen contained in a dewar with CaF_2 windows.

The solvents used in the spectroscopic studies, 1,2-

epoxyethylbenzene were obtained from Aldrich and used without further purification.

The light source used was a 100W high pressure mercury lamp filtered, in each case, with water contained in quartz. In some cases, filters with wavelengths between 320 and 400nm are used.

5.3 Typical photolysis procedures:

All photolysis processes are very similar. Here, I describe one example.

The complex cis-$CpW(CO)_2[P(nBu)_3]I$ was dissolved in 1,2-epoxyethylbenzene to produce a solution of optical density 0.5 for its most intense IR absorption band in the carbonyl region at $1942cm^{-1}$. This solution was then transferred into CaF_2 faced FTIR cells and cooled with the cryocooler to a temperature of 12K and allowed to equilibrate. The sample was removed from the optical bench and irradiated with the water filtered output of a 100W Hg lamp for 1 minute. The FTIR was then recorded again and the procedure of photolysis record spectra was repeated until no further reaction occurred upon photolysis. Then, the compressor was turned off and the sample allowed to warm to about 100K and the FTIR spectra was recorded again until there is no further change in the spectra. The sample is then cooled back down to 12K without any photolysis and the FTIR spectra was recorded.

Solutions containing other compounds were repeated using the same procedure.

Reference:

1. R.Poli, *Organometallics*, **1990**, *9*, 1892.
2. M.S.Wrighton, *Chem. Rev.*, **1974**, *74*, 401.
3. A.N.Nesmeyanov, *Adv. Organometallic Chem.*, **1972**, *12*, 56.
4. R.J.Kinney; W.D.Jones; R.G.Bergman, *J. Am. Chem. Soc.*, **1978**, *100*, 7902.
5. E.O.Fischer; R.J.J.Schneider, *Angew. Chem. Int. Ed. Engl.*, **1968**, *7*, 136.
6. D.G.Alway; K.W.Barnett, *Inorg. Chem.*, **1980**, *19*, 779.
7. P.Kubacek; R.Hoffman; Z.Havlas, *Organometallics*, **1982**, *1*, 180.
8. J.G.Calvert; J.N.Pitts,Jr., *Photochemistry*, **1967**, p19, Wiley, New York.
9. G.J.Ferraudi, *Elements of Inorganic Photochemistry*, **1988**, p8, Wiley, New York.
10. G.J.Ferraudi, *Elements of Inorganic Photochemistry*, **1988**, p80, Wiley, New York.
11. E.W.Abel; F.G.A.Stone, *Q. Rev. Chem. Soc.*, **1970**, *24*, 498.
12. A.Vogler, *Concepts in Inorganic Photochemistry*, **1975**, Chap. 6, A.W.Adamson and P.D.Fleischaner Eds., Wiley, New York.
13. G.J.Ferraudi, *Elements of Inorganic Photochemistry*, **1988**, p176, Wiley, New York.
14. J.K.Burdett, *Coor. Chem. Rev.*, **1978**, *27*, 1.
15. I.W.Stolz; G.R.Dobson; R.K.Sheline, *J. Am. Chem. Soc.*, **1962**, *84*, 3589; **1963**, *85*, 1013.
16. J.D.Black; M.J.Boylan; P.S. Braterman; W.J.Wallace, *J. Organometal. Chem.*, **1973**, *63*, C21.

17. J.D.Black; P.S.Braterman, *J. Organometal. Chem.*, **1973**, *63*, C19.

18. J.D.Black; P.S.Braterman, *J. Organometal. Chem.*, **1975**, *85*, C7.

19. M.A.Graham; P.N.Perutz; M.Poliakoff; J.J.Turner, *J. Oragnometal. Chem.*, **1972**, *34*, C34.

20. J.K.Burdett; M.A.Graham; R.N.Perutz; M.Poliakoff; A.J.Rest; J.J.Turner; R.F.Turner, *J. Am. Chem. Soc.*, **1975**, *97*, **4805**.

21. R.N.Perutz; J.J.Turner, *J. Am. Chem. Soc.*, **1975**, *14*, 262.

22. J.D.Black; P.S.Braterman, *J. Am. Chem. Soc.*, **1975**, *97*, 2908.

23. R.N.Perutz; J.J.Turner, *J. Am. Chem. Soc.*, **1975**, *97*, 4791.

24. J.K.Burdett; R.N.Perutz; M.Poliakoff; J.J.Turner, *J. Chem. Soc. Chem. Commun.*, **1975**, 157.

25. M.D.Adams; A.Square, *J. Organometal. Chem.*, **1973**, *63*, 381.

26. P.Legzdins; S.J.Rettig; L.Sanchez, *Organometallics*, **1988**, 7, 2397.

27 R.H.Hill; B.J.Palmer, *J.Organomallics*, **1989** , *8*, 1651.

28. J.D.Debad; R.H. Hill, *Can. J. Chem.*, in press.

29. F.A.Cotton; C.S.Kraihanzel, *J. Am. Chem. Soc.*, **1962**, *84*, 4432.

30. C.S.Kraihanzel; F.A.Cotton, *Inorg. Chem.*, **1963**, *2*, 533.

31. F.A.Cotton, *Inorg. Chem.*, **1964**, *3*, 702.

32. J.A.Timney, *Inorg. Chem.*, **1979**, *9*, 2502.

33. R.Hoffmann, *J. Chem. Phys.*, **1963**, *29*, 1379.

34 D.Rehder, *J. Magnetic Resonance*, **1977**, *25*, 177.

35. M.J.Mays; S.M.Pearson, *J. Chem. Soc. (A)*, **1968**, 2291.

36. S.Komiya; T.A.Albrigh; R.Hoffman; J.K.Kochi, *J. Am. Chem. Soc.*, **1976**, *10* 7255.

37. R.B.King; R.H.Reimann, *Inorg. Chem.*, **1980**, *15*, 183.

38. D.G.Alway; K.W.Barnett, *Inorg. Chem.*, **1980**, *19*, 1533.

39. D.L.Beach; K.W.Barnett, *J. Organometal. Chem.*, **1975**, *97*, C27.

40. R.B.Hitam; A.J.Rest, *Organometallics*, **1989**, *8*, 1598.

41. M.Elian; R.Hoffman, *Inorg. Chem.*, **1975**, *14*, 1058.

42. P.Hoffman, *Angew. Chem. Int. Ed. Engl.*, **1977**, *16*, 536.

43. J.Dalton; I.Paul; F.G.Stone, *J. Am. Chem. Soc.*, **1974**, *96*, 4998.

44. O.Crichton; A.T.Rest; D.J.Talor, *J. Chem. Soc., Dalton Trans.*, **1980**, 167.

45. N.J.Fitzpatrick; A.T.Rest; D.J.Talor, *J. Chem. Soc., Dalton Trans.*, **1979**, *46*, 351.

46. G.C.Faber; R.angelici, *J. Inorg. Chem.*, **1970**, *9*, 1586.

47. R.B.King; L.W.Howk, *Can. J. Chem.*, **1969**, *47*, 2959.

48. L.J.Todd; J.R.Wilkinson; J.P.Hickey; D.L.Beach; K.W.Barnett, *J. Organometallic Chem.*, **1978**, *151*, 154.

49. H.B.Abrahamson; M.C.Palazzotto; C.L.Reiche; M.S.Wrighton, *J. Am. Chem.Soc.*, **1979**, *101*, 4123.

50. P.S.Braterman, *Structure and Bonding*, **1972**, *10*, 57.

51. B.J.Ransil, *Rev. Mod. Phys.*, **1960**, *32*, 245.

52. F.A.Cotton, *Modern Coordination Chemistry*, **1960**, p301, J. Lewis; R.G.Wilkins Eds., Interscience, New York.

53. F.A. Cotton; C.S.Kraihanzel, *Inorg. Chem.*, **1962**, *2*, 4432.

54. J.K. Burdett; M.Poliakoff; J.J.Turner, *Adv. Infrared and Raman Spectroscopy*, **1976**, *2*, 1.

55. P.S.Braterman, *Metal Carbonyl Spectra*, **1975**, Academic Press, Lodon.

56. J.K.Burdett, *Coord. Chem. Rev.*, **1978**, *27*, 1.

57. J.K.Burdett, *Inorg. Chem.* , **1981**, *20*, 2607.

58. H.Haas; R.K.Sheline, *J. Chem. Phys.*, **1967**, *47*, 2996.

59. M.Moskovits; G.A.Oziu, *Vibrational Spectra and Structure*, **1976**, J.Durig. Ed., Elsevier, Amsterdam.

60. R.J.H.Clark, *J. Organomet. Chem.*, **1966**, *6*, 167.

61. This program was created by J.A. Craston and C.G.Brinkley at M.I.T. in Feb. 1986.

62. D.J. Darensbourg; M.Y. Darensbourg, *Inorg. Chem.*, **1970**, *9*, 1691.

63. R.C.Bush; R.J. Angelici, *J. Am. Cnem. Soc.*, **1986**, *108*, 2735.

64. B.E. Bursten; M.R.Green, *Progress in Inorg. Chem.*, V36, 393.

65. K.Yates, *Huckel Molecular Orbital Theory*, **1978**, p27, Academic Press, New York.

66. S.Komiya; T.A.Albright; R.Hoffmann; J.K.Kochi, *J. Am. Chem. Soc.*, **1976**, 7255.

67. M.Elian; R.Hoffmann, *Inorg. Chem.*, **1975**, *14*, 1058.

68. K.Yates, *Huckel Molecular Orbital theory*, **1978**, p190, Academic Press, New York.

69. J.C.Slater, *Phys. Rev.*, **1930**, *36*, 57.

70. M.Wolfsherg; L.Helmholtz, *J. Chem. Phys.*, **1952**, *20*, 837.

71. T.A.Albright, P.Hofmann; R.Hoffmann, *J. Am. Chem. Soc.*, **1977**, *23*, 7546.

72. J.H.Ammeter; H.B.Burgi; J.C.Tibeault; R.Hoffmann, *J. Am. Chem. Soc.*, **1978**, *100*, 3686.

73. R.Kubacek; R.Hoffmann; Z.Havlas, *Organometallics*, **1982**, *1*, 180.

74. R.Hoffmann, *Science*, **1981**, *211*, 995.

75. J.K.Burdett, *ibid*, **1975**, *14*, 375.

76. J.K.Burdett, *J. Chem. Soc., Faraday Trans. II*, **1975**, *70*, 1599.

77. A.D.Walsh, *J. Chem. Soc.*, **1950**, 2260.

78. R.Hoffmann, *J. Chem. Phys.*, **1963**, *39*, 1397.

79. R.H.Summerville; R.Hoffmann, *J. Am. Chem. Soc.*, **1976**, *98*, 7240.

80. D.Rehder; I.Muller; J.Kopf, *J. Inorg. Nucl. Chem.*, **1978**, *40*, 1013.

81. B.Sessen; T.H.Lemmen; H.J.C.Luttikhedde; J.H.Teuben; J.L.Petersen; J.C.Huffman; S.Jagner; K.G.Caulton, *Organometallics*, **1987**, *6*, 2354.